

**BEHAVIOURAL MODELING OF DYNAMIC
NONLINEAR TRANSMITTERS FOR LTE-ADVANCED
APPLICATIONS**

BY

Mohammed Hanzala Suleman Khan

A Thesis Presented to the
DEANSHIP OF GRADUATE STUDIES

KING FAHD UNIVERSITY OF PETROLEUM & MINERALS

DHAHRAN, SAUDI ARABIA

In Partial Fulfillment of the
Requirements for the Degree of

MASTER OF SCIENCE

In

ELECTRICAL ENGINEERING

April 2014

KING FAHD UNIVERSITY OF PETROLEUM & MINERALS

DHAHRAN- 31261, SAUDI ARABIA

DEANSHIP OF GRADUATE STUDIES

This thesis, written by **MOHAMMED HANZALA SULEMAN KHAN** under the direction his thesis advisor and approved by his thesis committee, has been presented and accepted by the Dean of Graduate Studies, in partial fulfillment of the requirements for the degree of **MASTER OF SCIENCE IN ELECTRICAL ENGINEERING.**



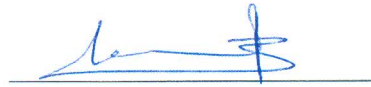
Dr. Ali Ahmad Al-Shaikhi
Department Chairman



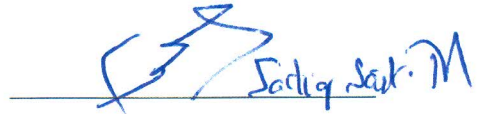
Dr. Salam A. Zummo
Dean of Graduate Studies

Date

11/5/14



Dr. Oualid Hammi
(Advisor)



Dr. Sadiq M. Sait
(Member)



Dr. Khurram K. Qureshi
(Member)

© Mohammed Hanzala Suleman Khan

2014

Dedicated to my

Parents and siblings

ACKNOWLEDGEMENTS

All praise be to Allah, *subhanahu-wa-ta'ala*, the Almighty who gave me the opportunity to pursue the MS degree course at King Fahd University of Petroleum and Minerals, and guided me in every facet of this work to help accomplish it successfully. May the peace and blessings of Allah be upon his prophet, Muhammad (S.A.W).

Acknowledgement is due to the King Fahd University of Petroleum and Minerals for providing the financial support and world class facilities in academic and extra-curricular activities.

I would like to express my appreciation to many people whose help, directly or indirectly, made this thesis work possible. With deep and indebted sense of gratitude, I would like to express my sincere thanks to my thesis advisor, Dr. Oualid Hammi for his invaluable support, guidance, continuous encouragement and every possible cooperation throughout the period of my research and preparation of thesis documentation. Working with him was a wonderful and learning experience, which I thoroughly enjoyed. A special note of acknowledgement to the iRadio Laboratory, University of Calgary for their support and assistance in providing the measurement data used in this work.

My sincere thanks and appreciation is due to the thesis committee members Dr. Sadiq Sait and Dr. Khurram Qureshi for investing their time and their support, critical reviews and suggestions which helped improve this work. I would like to acknowledge the Center for Communications and Information Technology Research, Research Institute, KFUPM, and all the staff therein, for providing me the Research Assistant

position during the tenure of my master's program. Working on different activities at the Center helped me grow on both professional and personal levels.

I am grateful to all the faculty and staff of the Electrical Engineering department, who have in one way or other enriched my academic and research experience at KFUPM. I owe a deep sense of gratefulness to my numerous friends and colleagues whose presence and moral support made my entire stay at KFUPM enjoyable and fruitful. I would like to sincerely thank them all, especially Tayyab Mujahid, Abderezak, Asim bhai, Najam bhai, Romman bhai and Osman.

Finally, I would like to express my profound gratitude to my parents, my siblings and all family members for their constant inspiration, incessant prayers, love, support and encouragement that motivated me to complete this work.

TABLE OF CONTENTS

ACKNOWLEDGEMENTS.....	v
TABLE OF CONTENTS.....	vii
LIST OF TABLES.....	x
LIST OF FIGURES.....	xi
LIST OF ABBREVIATIONS.....	xiii
ABSTRACT.....	xiv
ABSTRACT (ARABIC).....	xvi
CHAPTER 1 INTRODUCTION.....	1
1.1 Long Term Evolution (LTE) and LTE-Advanced	2
1.2 RF Power Amplifier Technologies.....	4
1.3 Behavioral Modeling and Digital Predistortion	6
1.4 Static Nonlinearity and Memory Effects	8
1.5 Problem Description.....	9
1.6 Contribution	10
1.7 Thesis Organization	11
CHAPTER 2 Literature Review: RF Power Amplifier Behavioral Models.....	12
2.1 Wiener and Hammerstein Models	12
2.1.1 Wiener Model	12
2.1.2 Hammerstein Model	13
2.1.3 Augmented Wiener Model	14

2.1.4	Augmented Hammerstein Model	15
2.2	Polynomial Based Models	16
2.2.1	Memoryless/ Look-Up-Table Model	16
2.2.2	Memory Polynomial Model	17
2.2.3	Envelope Memory Polynomial Model.....	18
2.2.4	Hybrid MP-EMP (HMEM) Model.....	19
2.2.5	Generalized Memory Polynomial Model (GMPPM).....	20
2.2.6	Nonuniform Memory Polynomial Model.....	21
2.3	Twin Nonlinear Two-Box Models	22
2.4	Parallel LUT-MP-EMP Model	23
2.5	Generalized TNTB Model.....	24
2.6	Volterra Series Based Models	25
2.6.1	Volterra Model	25
2.6.2	Dynamic Deviation Reduction (DDR) Based Volterra Model	26
2.6.3	DDR Volterra Model with Fading Memory.....	29
2.7	Complexity Evaluation of PA Behavioral Models	30
CHAPTER 3 Behavioral Models' Assessment Metrics		32
3.1	Normalized Mean Square Error.....	33
3.2	Memory Effects Ratio and Memory Effects Modeling Ratio	33
3.3	Adjacent Channel Error Power Ratio and Weighted Error-to-Signal Power Ratio	34
3.4	Memory Effects Intensity	35
3.5	Measurement Set-up	36

3.6	Application of Assessment Metrics for Memory Polynomial Model Dimension Estimation	40
3.6.1	Nonlinearity order estimation	41
3.6.2	Memory depth estimation	42
3.6.3	Conclusion	44
CHAPTER 4 Hybrid Twin Nonlinear Two-Box Model		46
4.1	Proposed Hybrid Twin Nonlinear Two-Box (HTNTB) Model.....	47
4.2	Model Identification.....	49
4.2.1	FTNTB model identification.....	50
4.2.2	ATNTB model identification	52
4.2.3	HTNTB model identification.....	53
4.3	Sequential method for HTNTB model identification	56
4.3.1	Augmenting the Memory Polynomial Function	57
4.3.2	Augmenting the Envelope Memory Polynomial Function	60
4.4	Comparative Analysis of HTNTB Model Identification	62
CHAPTER 5 Conclusion and Future Work		65
References		69
Vitae.....		74

LIST OF TABLES

Table 2.1 Complexity of the different models	31
Table 3.1 Model performance of the DUTs.....	42
Table 3.2 Memory depth of the DUTs.....	43
Table 3.3 MEI values of the DUTs.....	44

LIST OF FIGURES

Figure 1.1 Example of Carrier Aggregation	4
Figure 1.2 Concept of black box based behavioral modeling.....	8
Figure 2.1 Block diagram of the Wiener model	13
Figure 2.2 Block diagram of the Hammerstein model.....	13
Figure 2.3 Block diagram of the augmented Wiener model.....	15
Figure 2.4 Block diagram of the augmented Hammerstein model	15
Figure 2.5 Block diagram of the look-up-table model.....	16
Figure 2.6 Block diagram of the memory polynomial model.....	17
Figure 2.7 Block diagram of the envelope memory polynomial model	18
Figure 2.8 Block diagram of the hybrid MP-EMP (HMEM) model	20
Figure 2.9 Block diagram of the forward TNTB model	22
Figure 2.10 Block diagram of the reverse TNTB model	22
Figure 2.11 Block diagram of the parallel TNTB model.....	22
Figure 2.12 Block diagram of the PLUME model.....	24
Figure 2.13 Block diagram of the generalized TNTB model	24
Figure 2.14 Block diagram of the Volterra model.....	26
Figure 3.1 Comparison of measured and model output.....	33
Figure 3.2 Measurement setup for PA characterization.....	37
Figure 3.3 AM/AM and AM/PM characteristics of DUT (a) raw data (b) time aligned data.....	38
Figure 3.4 DUT 1 characteristics (a) AM/AM characteristics and (b) AM/PM characteristics.....	39

Figure 3.5 DUT 2 characteristics (a) AM/AM characteristics and (b) AM/PM characteristics	39
Figure 3.6 DUT 3 characteristics (a) AM/AM characteristics and (b) AM/PM characteristics	40
Figure 3.7 Block diagram for the memoryless post-compensation technique.....	41
Figure 4.1 Block Diagram of the augmented twin nonlinear two-box model	47
Figure 4.2 Block diagram of the proposed hybrid twin nonlinear two-box model.....	49
Figure 4.3 FTNTB model performance for the 60MHz LTE-A signal	51
Figure 4.4 FTNTB model performance for 60MHz LTE-A signal as a function of nonlinearity order and memory depth	51
Figure 4.5 ATNTB model performance for the 60MHz LTE-A signal.....	52
Figure 4.6 HTNTB model performance for the 60MHz LTE-A signal.....	53
Figure 4.7 NMSE versus number of coefficients for the 60MHz LTE-A signal.....	54
Figure 4.8 NMSE versus number of coefficients for the 80MHz LTE-A signal.....	55
Figure 4.9 NMSE performance of the augmented memory polynomial function for (a) 60MHz LTE-A signal and (b) 80MHz LTE-A signal.....	59
Figure 4.10 NMSE performance of the augmented envelope memory polynomial function for (a) 60MHz LTE-A signal and (b) 80MHz LTE-A signal.....	61
Figure 4.11 Comparative Analysis of HTNTB Model Identification for (a) 60MHz signal and (b) 80MHz LTE-A signal	63

LIST OF ABBREVIATIONS

LTE-A	Long Term Evolution – Advanced
DPD	Digital Predistortion
DUT	Device Under Test
PA	Power Amplifier
PAPR	Peak to Average Power Ratio
LDMOS	Laterally Diffused Metal Oxide Semiconductor
MP	Memory Polynomial
EMP	Envelope Memory Polynomial
TNTB	Twin Nonlinear Two-Box
HMEM	Hybrid Memory Polynomial - Envelope Memory Polynomial
NMSE	Normalized Mean Square Error
HTNTB	Hybrid Twin Nonlinear Two-Box
ATNTB	Augmented Twin Nonlinear Two-Box

ABSTRACT

Full Name : Mohammed Hanzala Suleman Khan
Thesis Title : Behavioural Modeling of Dynamic Nonlinear Transmitters for LTE-Advanced Applications
Major Field : Electrical Engineering
Date of Degree : April 2014

The Long Term Evolution (LTE) and LTE-Advanced (LTE-A) standards for wireless mobile communication are now being commercially available in many countries to increase the capacity and speed of wireless telecommunication networks. They are characterized by wideband signals having a non-constant envelope leading to high peak-to-average power ratio (PAPR). Moreover, the base station power amplifier (PA) is an important component of the radio base station as it uses a considerable amount of the power consumed by the entire network. Hence, its efficient performance and linear operation are absolutely essential. Employing signals with high PAPR stimulates the nonlinear behaviour of the PA whereas operating the PA in its linear region results in significant loss of efficiency. Therefore, it is essential to achieve efficient trade-off between linearity and efficiency. Behavioral modeling of radio frequency (RF) PAs has thus attracted the interest of many researchers and has proved to be valuable for digital predistortion which is an important technique to help improve the efficiency of the amplifier while maintaining its linear behavior. An important aspect in behavioral modeling application is selecting an appropriate model that will be able to precisely depict the PA performance. In order to assess the performance and accuracy of a behavioral model various performance evaluation metrics have been studied. A novel

technique for identifying the dimensions of the memory polynomial model has been proposed. A new class of behavioral models built on the conventional twin nonlinear two-box models is proposed for power amplifiers driven by wideband LTE-A signals. The conventional forward twin nonlinear two-box (FTNTB) model structure improves the modeling accuracy of the memory polynomial model whereas the hybrid memory polynomial-envelope memory polynomial (HMEM) model gives better modeling performance when the amplifier is driven by wideband signals. The proposed model, labeled hybrid twin nonlinear two-box (HTNTB) model thus combines the advantages of the FTNTB model and the HMEM model. Its performance is benchmarked against the conventional FTNTB model and previously reported augmented twin nonlinear two-box (ATNTB) model. Experimental results validated on 300W Laterally Diffused Metal Oxide Semiconductor (LDMOS) based Doherty amplifier operating at 2140MHz demonstrate the ability of the HTNTB model to considerably outperform the conventional FTNTB model in terms of performance and the ATNTB models in term of complexity reduction.

ABSTRACT (ARABIC)

ملخص الرسالة

الاسم الكامل: محمد حنظله سليمان خان

عنوان الرسالة: النمذجة السلوكية للمرسل ذو الاداء غير الخطي المتغير لتطبيقات اتصالات الجيل الرابع

التخصص: الهندسة الكهربائية

تاريخ الدرجة العلمية: أبريل 2014

الجيل الرابع من تكنولوجيا الاتصالات (LTE) & (LTE-A) اصبح الان متاحا في غالبية الدول حول العالم على المستوى التجاري لرفع اداء وجوده الاتصالات في الشبكات اللاسلكية. هذا الجيل من تكنولوجيا الاتصالات يعتمد على الاشارات ذات النطاق العريض التي تحمل نسبة طاقة كبيرة مقارنة مع معدل الطاقة التي تحتويها (PAPR). يعتبر مكبر الطاقة في المحطة الاساسية في الشبكة من اهم المكونات حيث انه يستهلك معظم الطاقة في الشبكة. بناء على ذلك فان فاعليته وادائه يعتبر شديد الاهمية بالنسبة للشبكة ككل. التعامل مع الاشارات التي نسبة طاقة كبيرة مقارنة مع معدل الطاقة التي تحتويها يؤدي الى اداء غير خطي ينتج عنه هبوط في الاداء الخاص بمكبر الاشارة. لذلك في انه من المهم الحصول على توازن مقبول بين فاعلية الاداء وخطية العلاقة.

النمذجة السلوكية لمكبر الطاقة لفتت نظر الباحثين وحازت على اهتمامهم في الفترة الاخيرة وأثبتت انها قادرة على ان تكون مفيدة بالنسبة لدائرة تقليل التشويه الرقمية التي تحسن الاداء وتحافظ على خطية العلاقة. الشيء المهم في النمذجة السلوكية هو اعطاء وصف رياضي دقيق للعلاقة بين المدخل والمخرج لمكبر الطاقة. لمعرفة مدى صلاحية النماذج المقترح فان هناك عدد من مؤشرات الاداء تم دراستها في هذا الرسالة. لقد تم اقتراح طريقة جديدة لحساب ابعاد النموذج متعدد الحدود ذو الذاكرة.

طبقة جديدة من النماذج السلوكية تم بناؤها بالاعتماد على نموذج التوأم الغير خطي ثنائي المربع المطبق على اشارات الجيل الرابع من الاتصالات اللاسلكية. النموذج الامامي للتوأم الغير خطي ثنائي المربع العادي (FTNTB) يحسن من دقة النمذجة, في المقابل فإن النموذج الهجين المتعدد الحدود ذو الذاكرة (HMEM) يعطي اداء أفضل حال استخدامه مع الاشارات ذات النطاق العريض.

النموذج المقترح، يسمى النموذج الهجين للتوأم الغير خطي ثنائي المربع (HTNTB) الذي هو عبارة عن نموذج يجمع بين حسنات النموذج الامامي للتوأم الغير خطي ثنائي المربع (ATNTB) والنموذج الهجين المتعدد الحدود ذو الذاكرة. أداء هذا النموذج الجديد تمت مقارنته مع النموذج الامامي للتوأم الغير خطي ثنائي المربع والنموذج الزائد للتوأم الغير خطي ثنائي المربع. نتائج التجربة أختبرت على مكبر طاقة يعتمد على اشباه الموصلات (LDMOS) يعمل ب 300 واط على تردد 2140 ميغاهرتز وقد أظهرت أن النموذج المقترح اعطى أداء أفضل من النموذج الامامي للتوأم الغير خطي ثنائي المربع بالنسبة للأداء وأفضل من النموذج الزائد للتوأم الغير خطي ثنائي المربع بالنسبة لتقليل الصعوبة.

CHAPTER 1

INTRODUCTION

Communication between humans played a vital role in the emergence and development of civilizations. Without inter-human communications, civilization could not have amassed the wealth of knowledge that is now readily available at our disposal and the world would have been a very primitive place. Methods of communication between humans have continuously evolved over centuries. Progressively, newer technologies have been developed for the transmission of information in a clear, effective and efficient manner.

The need and the desire to develop a system for broadcasting information over longer distances resulted in the invention of electrical communications which revolutionized the art of transmission and distribution of information. In this regard, Samuel Morse (1837), Bell (1887) and Marconi (1898) are regarded as the pioneers of electrical communications. The invention of telegraph by Morse played a major role in long range digital communications using electrical transmission wires, and was first used in railways in the United States. This mode of communication was faster than any other means of communications known before. Alexander Graham Bell invented the telephone to communicate interactively over distances where traditional voice communications was not possible. Marconi was responsible for long range radio communications which revolutionized the distribution of information by means of international broadcasting. In

the 20th century, cellular mobile communication systems have evolved which mark the beginning of wireless communication. Wireless communication systems have advanced rapidly in the past couple of decades. The number of consumers using mobile network services has increased multiple times since the technology first became available for commercial use. There is growing competition among the mobile service providers and in order to attract more customers various features and services are being offered. Numerous mobile base stations are being constructed in order to meet this ever growing demand. Mobile base stations are basically a part of the network that transmits and receives radio signals to create a connection between the dialer and the receiver. With the development of smart phones and tablets the amount of information transmitted across these networks has extensively increased. Therefore, it is crucial for the base station PA to work efficiently. An introduction to Long Term Evolution (LTE) and LTE-Advanced communication technologies, the different power amplifier technologies, the concept of behavioral modeling and digital predistortion, static nonlinearity and memory effects are described in this chapter.

1.1 Long Term Evolution (LTE) and LTE-Advanced

LTE which stands for Long Term Evolution has been developed by the 3rd Generation Partnership Project (3GPP) international standard organization. LTE is a standard for wireless data communications technology and an advancement of the Global System for Mobile Communications (GSM) and Universal Mobile Telecommunications System (UMTS) standards [1]. The motive of developing LTE was to increase the speed and capacity of wireless data networks. Even though LTE was initially proposed by one of the leading mobile phone operators NTT DoCoMo in Japan, 2004, this technology was

first made commercially available to the public in Stockholm (Sweden) and Oslo (Norway) in year 2009 and followed by Japan and United States in 2010 [1] [2]. Peak downlink rates of 300 Mbps and uplink rates of 75 Mbps is provided by the LTE Release 8 specification and it also supports multiple scalable bandwidths including 1.4, 3, 5, 10, 15 and 20 MHz [1]. Mobile service providers across the globe have now started providing LTE network and many mobile devices supporting LTE have been launched in recent years. LTE (Release 8) could not meet the requirements set by International Telecommunication Union (ITU) for International Mobile Telecommunications-Advanced (IMT Advanced), also referred to as 4G. Thus, LTE-Advanced (Release 10) which is an evolution of LTE (Release 8 and 9) was developed to provide much higher data rates in a cost efficient way and, at the same time, completely fulfil the requirements set by ITU for IMT Advanced [1]-[3]. LTE-Advanced also offers full backward compatibility with earlier versions of LTE. Peak data rates of 3Gbps in downlink and 1.5 Gbps in uplink, higher spectral efficiency, increased number of simultaneously active subscribers and carrier aggregation (CA) are some of the important features of LTE-Advanced. Extension of bandwidth in LTE-Advanced is achieved using carrier aggregation [3]-[5]. Individual component carriers can have bandwidth of 1.4, 3, 5, 10, 15 and 20 MHz and a maximum of 5 component carriers can be aggregated as shown in Figure 1.1 below [6]. Hence, upto 100 MHz bandwidth can be deployed. Carrier aggregation enables higher data rates and lower latencies for all users and helps provide more capacity for bursty applications like web browsing often used in many smart phones. According to recent Global mobile Suppliers Association (GSA)'s "Evolution to LTE Report"[7] LTE Market Summary, 274 LTE networks have already been

commercially launched in 101 countries and it has been one of the fastest mobile system technology ever to be developed so far. In few years' time LTE and LTE-Advanced together are expected to become the globally used standard for mobile communication.

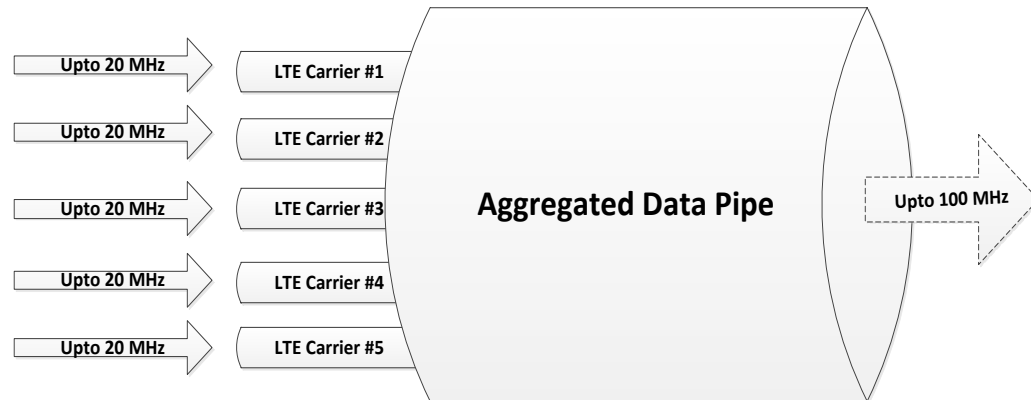


Figure 1.1 Example of Carrier Aggregation

1.2 RF Power Amplifier Technologies

Amplifier is a device designed to increase the input signal power levels. The basic principle of operation is that it takes energy from the power supply and controls the output to match the shape of the input signal but with higher amplitude. Therefore, fundamentally an amplifier modulates the power supply output. Different types of amplifiers are available specially designed for different requirements and applications.

A power amplifier is usually the final amplification stage in a system, designed to give the required output power. From communications systems perspective, power amplifiers are mainly present in transmitters and are specifically designed to raise the input signal power level before passing it to antenna. Having this power boost is fundamental for the desired signal to noise ratio to be achieved on the receiver end, without which it will be difficult to detect the received signal.

It is necessary for the power amplifier to have as high efficiency as possible while at the same time maintaining linearity i.e. adding as little distortion to the signal as possible. High power efficiency is of prime importance in small and mobile transmitters, since these devices are usually driven by battery. It is also important for base stations as it affects their deployment and operating costs as well as their carbon foot print. Unfortunately, from circuit design view point if the power efficiency is increased the device is driven more and more into the nonlinear region thus increasing the amount of distortion. Accordingly, efficiency and linearity considerations lead to various classes of power amplifiers such as class A, class B, class AB, class C, etc.

Class A is the most linear but most inefficient of all power amplifier designs having about 20% efficiency. Class B amplifiers create large amount of distortions but have a maximum theoretical efficiency of 78.5%. Class AB is less efficient than class B but achieves more linearity. Class C amplifiers are nonlinear amplifiers but high efficiencies (up to 90%) are achievable. RF PAs enabled by various semiconductor technologies are vital components in any of the wireless communication systems. For the wireless systems to comply with ITU (International Telecommunication Technologies) regulations, these amplifiers must meet strict performance specifications of output power and linear operation in addition to other requirements including its reliability, robustness, cost and physical size set by the manufacturers. RF PAs are designed using a wide variety of semiconductor technologies. Si BJT, Si LDMOS FET, SiGe HBT and GaN are some of these technologies [8]. The Laterally Diffused Metal Oxide Semiconductor (LDMOS) technology is generally used for RF power amplifiers employed in wireless communication network base-stations in order to satisfy the requirement of high output

power. However, the efficiency of LDMOS devices is severely affected because of the use of signals with high peak-to-average power ratio (PAPR) used in most of the advanced wireless communication networks. The efficiency of the power amplifiers can be enhanced by means of Doherty or Envelope Tracking techniques.

William H. Doherty invented the Doherty Amplifier in 1934 for Bell Laboratories. It was originally constructed using vacuum tubes. The Doherty amplifier consists of a main amplifier and an auxiliary amplifier connected in such a way that the combination boosts the power efficiency of the main amplifier. High efficiency, ease of implementing the linearization methods and simplicity are some of the advantages of the Doherty power amplifiers. Doherty amplifier prototype is used as the device under test (DUT) in the experiments performed in this work.

1.3 Behavioral Modeling and Digital Predistortion

For improving the spectral efficiency, advanced wireless communication techniques like the third and fourth generation (3G and 4G) system, Worldwide Interoperability for Microwave Access (WiMAX), and Long Term Evolution (LTE) have been developed. These systems are continually evolving to support more number of users and provide better data rates within the available RF spectrum by transmitting maximum information using minimum spectrum space. Power amplifier plays an important part in the telecommunication network base station. It uses upto 75% of the power that is consumed by the entire network and hence its efficient operation and performance is absolutely necessary.

Due to the use of multicarrier modulations such as Orthogonal Frequency Division Multiplexing (OFDM) and Code Division Multiple Access (CDMA), signals

with high PAPR need to be handled by the transmitter and the power amplifier. High PAPR stimulates the nonlinear operation of a power amplifier which is inherently a nonlinear device. Hence, during the transmission process, some unwanted distortions such as degradation in bit error rate and spectral regrowth are caused. If the power amplifier is made to operate only in its linear region, there will be significant power efficiency loss. Therefore, over the past couple of decades most of the research in this regards has been on linearization of high power efficient PAs to improve the quality of communication without reducing the power efficiency. For achieving a tradeoff between linearity and efficiency, PA linearization technique is crucial.

Feedforward linearization technique provides extremely linear characteristics as proposed in [9] [10]. This technique however consists of complex control circuits and an auxiliary error power amplifier which increases the cost and degrades the efficiency. The feedback linearization technique proposed in [11] has the drawbacks of bandwidth limitation and instability. Among all the linearization techniques, the most extensively used technique is digital predistortion (DPD) for its high accuracy, flexibility and efficient operation [12]–[15].

Behavioral modeling and digital predistortion (DPD) are two important techniques that are used in order to solve the nonlinearity problem that is exhibited by the base station power amplifier. The idea is to have a digital predistorter, which typically has inverse characteristics of the PA, connected before the PA so that the two systems in cascade have a linear operation. This technique employs a black box based approach. As shown in Figure 1.2, behavioral modeling identifies a mathematical formulation relating the input and output signals of the amplifier. Having information about the radio frequency

circuitry of the PA is not required. Behavioral modeling provides a computationally efficient way to relate the input and output signals without performing any physical analysis of the system and is thus a valuable process for assessment of the transmitter performance and design of the digital predistorter [16] [17]. It is important to accurately obtain the DUT's input and output signals and the mathematical formulation should be able to describe all the important interactions that occur between these signals. This requires some apriori knowledge of the DUT.

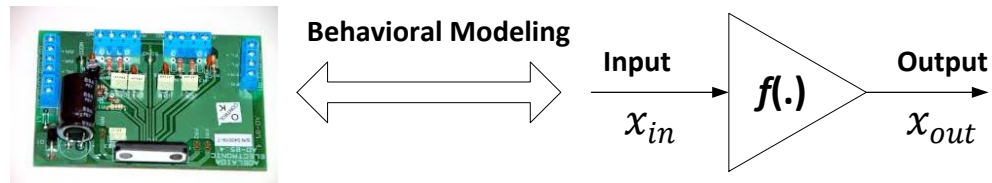


Figure 1.2 Concept of black box based behavioral modeling

1.4 Static Nonlinearity and Memory Effects

Two major factors which contribute to the nonlinear behavior of a power amplifier are static nonlinearity and memory effects. Static nonlinearity is more dominant among the two. Static nonlinearity, also known as memoryless nonlinearity, corresponds to the distortion produced by the DUT in the absence of memory effects. In this case, the output depends only on the actual input sample. Static distortions are generally represented by memoryless AM/AM and AM/PM characteristics. The device is said to exhibit memory effects, also known as dynamic distortions, when the output depends on the present input sample and a few number of past input samples. These memory effects can be either thermal or electrical. Electrical memory effects occur due to mismatch of

circuit impedance and passive components like resistors and capacitors and become more pronounced as signal bandwidth increases. Thermal memory effects arise due to temperature variation and are commonly observed for narrowband signals of around few hundred KHz. Static nonlinearity and memory effects of PAs and transmitters are affected by the characteristics of the signal such as signal average power, its bandwidth and PAPR. It has been observed that variations in signal average power influence the static nonlinearity of the DUT whereas with increase in bandwidth the memory effects become prominent [18] [19]. Because of the use of wide bandwidth signals in modern communication, behavioral models have to consider both of these effects.

1.5 Problem Description

The objective of behavioral modeling is to develop a model that will be able to mimic the nonlinear operation of the power amplifier while maintaining accuracy. In this regard, different behavioral models have been proposed in literature. For assessing the accuracy and performance of these models, there is a need for reliable and accurate metrics. Another important aspect that needs to be considered while selecting a model is its complexity. Dimensions of the model determine its size and complexity and hence accurately identifying the dimensions is essential. A lower model size affects the accuracy whereas complexity is increased if model size becomes large. Therefore, it is necessary to have an optimum process to select the best model size without compromising on accuracy. The memory polynomial (MP) model is one of the most commonly preferred behavioral models because of its simple structure and reliable performance. Memory depth (M) and nonlinearity order (N) are the dimensions of the

memory polynomial model. Using the performance evaluation metrics a novel technique for accurately identifying these dimensions has been proposed in this thesis work.

Modern mobile communication networks make use of LTE signals which are of wide bandwidth and high PAPR. These signal characteristics stimulate the static nonlinearity and the memory effects of the power amplifier wherein the power amplifier output is influenced by the actual input sample and also previous input samples. Behavioral models having a two-box structure such as the twin nonlinear two-box (TNTB) model depict both these distortions of the power amplifier effectively. However, there is further room for improvement in model performance without significantly increasing its complexity. This thesis work attempts to achieve this improvement by modifying the conventional TNTB model.

1.6 Contribution

This thesis work has two major contributions:

1. Using measured data, various time and frequency domain metrics have been evaluated to help determine the dimensions of the memory polynomial model. The post-compensation technique is found effective especially to help identify the memory effects of the PA. Measurements are performed using wideband long term evolution (LTE) signals on three power amplifier prototypes. The experimental results validate the generality and the validity of the proposed dimension estimation technique in avoiding unnecessary computational complexity caused by oversizing of the model dimension.
2. The hybrid twin nonlinear two-box (HTNTB) model has been proposed which significantly improves the performance of the conventional FTNTB model with reduced

complexity. The model performance is validated using LDMOS based Doherty amplifier driven by wideband LTE-A signals.

1.7 Thesis Organization

The thesis is covered in five chapters. The first Chapter introduces the area of the work and defines the problem addressed in this thesis. It includes an overview of LTE technology, RF power amplifiers, the principle of behavioral modeling and digital predistortion, the concept of static nonlinearity and memory effects, problem description and thesis contribution.

A thorough review of different behavioral models, alongwith their mathematical formulations, block diagrams and pros and cons is presented in Chapter 2. These models include the Wiener and Hammerstein based models, the memory polynomial based models, the two-box model structures, and the conventional Volterra and its simplified versions.

In Chapter 3, the various performance evaluation metrics are presented. The post-compensation technique, the measurement set-up, and the different DUTs used in the work are described. The methodology for identifying the dimensions of the memory polynomial model is discussed as well.

In Chapter 4, the HTNTB model is proposed and validated using Doherty power amplifier driven by LTE-A signals of 60MHz and 80MHz bandwidths. Its performance has been compared with that of the conventional FTNTB and ATNTB models. Conclusions are stated in Chapter 5.

CHAPTER 2

Literature Review: RF Power Amplifier Behavioral Models

Efficient and linear operation of RF power amplifiers is of prime importance as it is one of the most important component in wireless communication systems. Therefore, behavioral modeling, which attempts to predict the linearity performance of the power amplifier, has attracted the interest of many researchers over the past couple of decades. Because of the use of wide bandwidth signals, memory effects have become an essential part of power amplifier behaviour alongwith the static nonlinearity and cannot be ignored. Numerous models have been described in literature to depict the nonlinear behavior of power amplifiers driven by wide bandwidth signals. These structures include the memoryless look-up table model [20] [21], Hammerstein and Wiener models [22]–[26], memory polynomial (MP) model and its modifications [15], [27]–[32] , twin nonlinear two-box models [33], 3-box models such as PLUME model [34], generalized TNTB model [35], Volterra model and its variations [36]–[40]. Some of these models are based on separately identifying the static nonlinearity and memory effects.

2.1 Wiener and Hammerstein Models

2.1.1 Wiener Model

It is a two box model consisting of a linear finite impulse response (FIR) filter which is cascaded to a memoryless nonlinear function [23]. The Wiener model output is obtained as

$$x_{out}(n) = f_w[x_1(n)] \quad (2.1)$$

where $f_w[\cdot]$ is the memoryless nonlinear function and $x_1(n)$ is the FIR filter output given by

$$x_1(n) = \sum_{j=0}^M h(j) \cdot x_{in}(n-j) \quad (2.2)$$

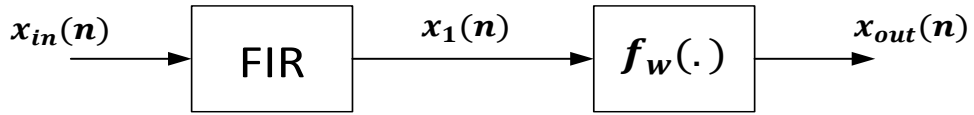


Figure 2.1 Block diagram of the Wiener model

M represents the memory depth of the DUT and $h(j)$ are the FIR filter impulse response coefficients. In the first step, the nonlinear function is identified. Then, by de-embedding the input and output waveforms of the FIR filter, the filter coefficients are identified.

2.1.2 Hammerstein Model

Hammerstein model is analogous to the Wiener model except that the static nonlinear function is cascaded before the linear filter [23].

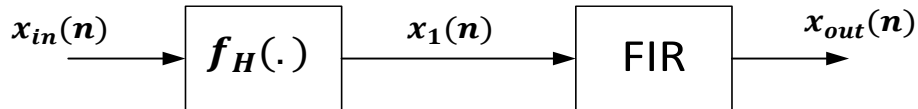


Figure 2.2 Block diagram of the Hammerstein model

The Hammerstein model output is given by

$$x_{out}(n) = \sum_{j=0}^M h(j) \cdot x_1(n-j) \quad (2.3)$$

and

$$x_1(n) = f_H[x_{in}(n)] \quad (2.4)$$

where $x_1(n)$ refers to the output of the memoryless nonlinear function $f_H[\cdot]$, $h(j)$ are the coefficients of the FIR filter, and M is the memory depth of the DUT.

2.1.3 Augmented Wiener Model

The Wiener and Hammerstein models fail to consider the nonlinearity contribution of memory effects which limits their performance. To overcome this drawback, the augmented versions of these models were developed which make use of multiple filters in cascade with the LUT model as shown in Figure 2.3 and Figure 2.4.

Formulation of Augmented Wiener model [25] output is similar to the conventional Wiener output and is obtained as

$$x_{out}(n) = f_w[x_1(n)] \quad (2.5)$$

where $f_w[\cdot]$ is the memoryless nonlinear function and $x_1(n)$ is the combined output of the multiple filters calculated using the instantaneous input baseband waveform $x_{in}(n)$.

$$x_1(n) = \sum_{i_1=0}^{M_1} h_1(i_1) \cdot x_{in}(n-i_1) + \sum_{i_2=0}^{M_2} h_2(i_2) \cdot x_{in}(n-i_2) \cdot |x_{in}(n-i_2)| \quad (2.6)$$

$h_1(i_1)$ and $h_2(i_2)$ are the impulse responses of the filters FIR1 and FIR2 and M_1 and M_2 are their memory depths respectively.

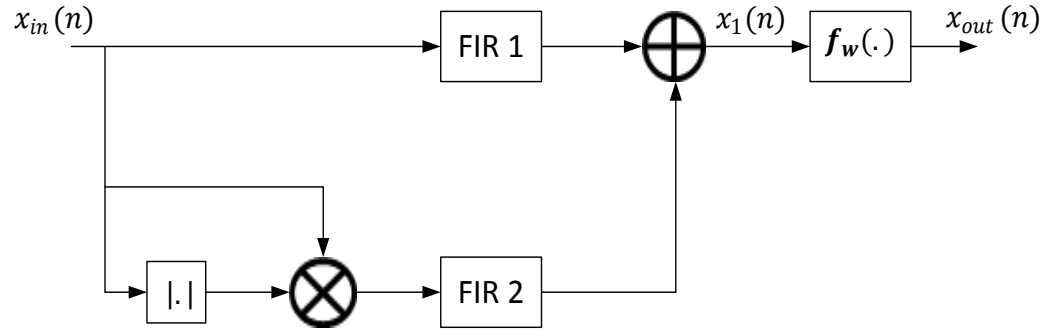


Figure 2.3 Block diagram of the augmented Wiener model

2.1.4 Augmented Hammerstein Model

The block diagram of the augmented Hammerstein model is shown in Figure 2.4.

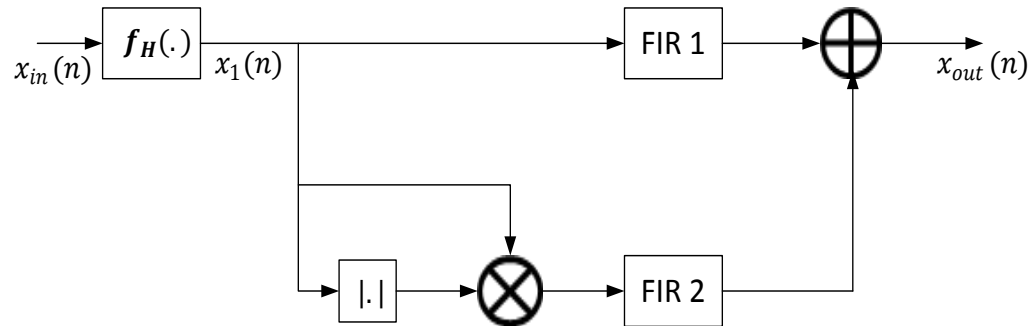


Figure 2.4 Block diagram of the augmented Hammerstein model

Using the same notations as used for the augmented Wiener model, the output $x_{out}(n)$ of the augmented Hammerstein model [26] is given as

$$x_{out}(n) = \sum_{i_1=0}^{M_1} h_1(i_1) \cdot x_1(n-i_1) + \sum_{i_2=0}^{M_2} h_2(i_2) \cdot x_1(n-i_2) \cdot |x_1(n-i_2)| \quad (2.7)$$

where,

$$x_1(n) = f_H[x_{in}(n)] \quad (2.8)$$

2.2 Polynomial Based Models

2.2.1 Memoryless/ Look-Up-Table Model

Figure 2.5 shows the memoryless look-up table (LUT) model. This LUT based behavioral model has been widely used in the past because it is easily implemented and is relatively simple [20]. This model does not include memory effects, and thus has a limited use now. In fact, currently, this model is used as a sub-model of more advanced structures that incorporate the memory effects of the power amplifier.

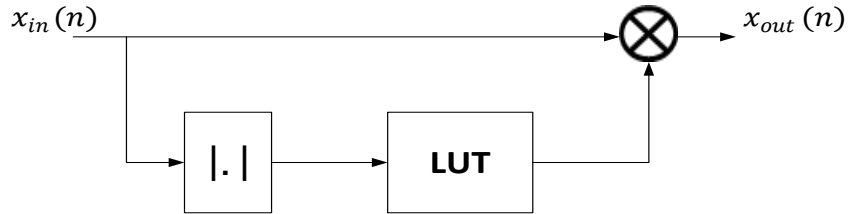


Figure 2.5 Block diagram of the look-up-table model

In the LUT model, the gain of the device under test is saved in the look-up table.

The LUT output is calculated as

$$x_{out}(n) = G[x_{in}(n)] \cdot x_{in}(n) \quad (2.9)$$

where $G[x_{in}(n)]$ represents the instantaneous gain of the DUT.

2.2.2 Memory Polynomial Model

Memory polynomial (MP) model [15] described in Figure 2.6 consists of several delay taps and nonlinear static functions. Because of its simple structure and high accuracy this model is extensively used for behavioral modeling and digital predistortion applications of power amplifiers that exhibit memory effects.

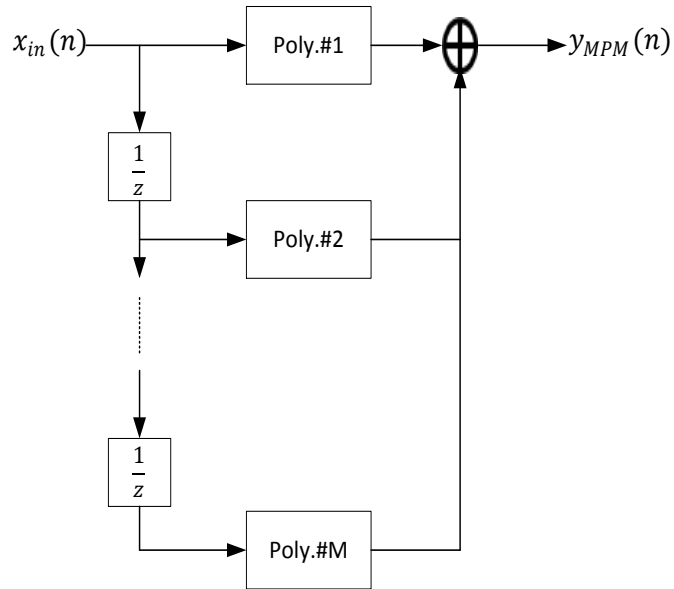


Figure 2.6 Block diagram of the memory polynomial model

The memory polynomial model is given by

$$y_{MPM}(n) = \sum_{j=1}^M \sum_{i=1}^N a_{ji} \cdot x_{in}(n+1-j) \cdot |x_{in}(n+1-j)|^{i-1} \quad (2.10)$$

where, $y_{MPM}(n)$ is the output of the memory polynomial model, $x_{in}(n)$ is the complex input signal, N is the nonlinearity order and M represents the memory depth of the

model. a_{ji} are the model coefficients which can be determined using least square approximation techniques. This model is a truncation of the Volterra model considering only the diagonal terms. The diagonal limitation significantly decreases the complexity, however it degrades model fidelity as in particular cases the off diagonal terms may influence the output in a significant manner [37]. Another disadvantage is that same nonlinear order is used in all the branches leading to oversized model which is undesirable [32] [41].

2.2.3 Envelope Memory Polynomial Model

The MP model uses the baseband complex input samples to determine its output whereas for envelope memory polynomial (EMP) model the output, $y_{EMPM}(n)$, depends on the absolute values of the previous baseband complex input samples $\left[|x_{in}(n)|, \dots, |x_{in}(n-M)|\right]$ and the actual baseband complex input sample $x_{in}(n)$.

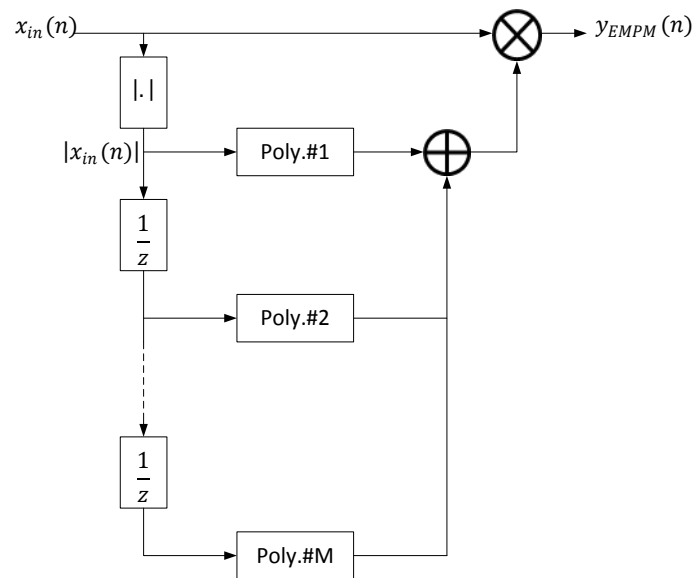


Figure 2.7 Block diagram of the envelope memory polynomial model

As proposed in [29] the baseband complex output sample for the EMP model is given by

$$y_{EMPM}(n) = x_{in}(n) \cdot \sum_{j=1}^M \sum_{i=1}^N a_{ji} \cdot |x_{in}(n+1-j)|^{i-1} \quad (2.11)$$

where, $y_{EMP}(n)$ is the output of the envelope memory polynomial model the other variables are the same as those defined in Equation (2.10). The envelope memory polynomial model shows good modeling performance especially when signals with zero carriers are employed [29].

2.2.4 Hybrid MP-EMP (HMEM) Model

Hybrid MP-EMP (HMEM) model combines the benefits of both memory polynomial and envelope memory polynomial models especially in the frequency domain [30]. The input signal $x(n)$ is fed to both models and their outputs are added to yield the overall output signal for the hybrid model. The output $y_{HMEM}(n)$ of the hybrid model is given by

$$\begin{aligned} y_{HMEM}(n) = & \sum_{j=1}^{M_{MP}} \sum_{i=1}^{N_{MP}} a_{ji} \cdot x(n+1-j) \cdot |x(n+1-j)|^{i-1} \\ & + \sum_{k=1}^{M_{EMPM}} \sum_{l=1}^{N_{EMPM}} b_{kl} \cdot x(n) \cdot |x(n+1-k)|^{l-1} \end{aligned} \quad (2.12)$$

where, M_{MP} and N_{MP} are the memory depth and the nonlinearity order of the MP model block of the hybrid model, respectively. While M_{EMPM} and N_{EMPM} are the memory depth and nonlinearity order of the EMP sub-model block, respectively. By addition of a few number of coefficients, this model is able to effectively improve the modeling

accuracy of the memory polynomial model especially when nonlinear power amplifiers exhibiting strong memory effects are driven by multicarrier signals.

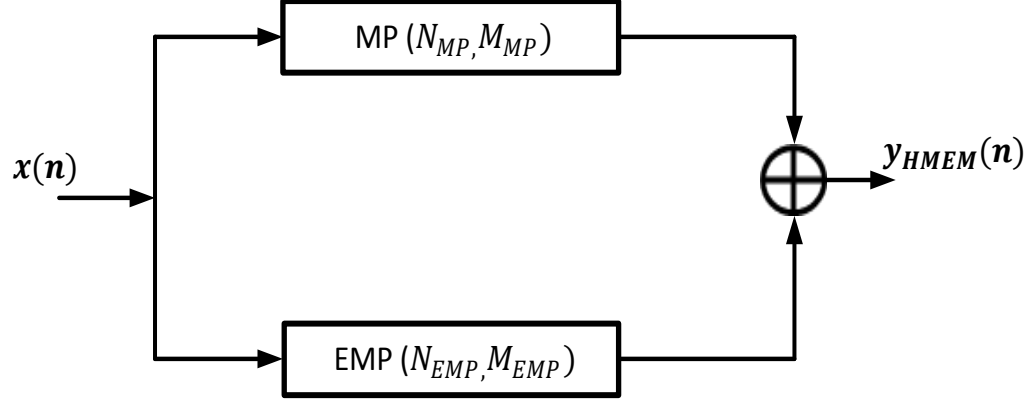


Figure 2.8 Block diagram of the hybrid MP-EMP (HMEM) model

2.2.5 Generalized Memory Polynomial Model (GMPM)

Combining the memory polynomial model in Equation (2.10) with cross terms between the signal and leading/lagging envelope terms results in the generalized memory polynomial model [31] described as

$$\begin{aligned}
 y_{GMP}(n) = & \sum_{k=0}^{N_a-1} \sum_{m=0}^{M_a-1} a_{km} \cdot x(n-m) |x(n-m)|^k \\
 & + \sum_{k=1}^{N_b} \sum_{m=0}^{M_b-1} \sum_{l=1}^{L_b} b_{kml} \cdot x(n-m) |x(n-m-l)|^k \\
 & + \sum_{k=1}^{N_c} \sum_{m=0}^{M_c-1} \sum_{l=1}^{L_c} c_{kml} \cdot x(n-m) |x(n-m+l)|^k
 \end{aligned} \tag{2.13}$$

Here, $x(n)$ and $y_{GMP}(n)$ are the input and output signals of the generalized memory polynomial model respectively. a_{km}, b_{kml}, c_{kml} represent the model coefficients of the MP branch, lagging effect branch and leading effect branch, respectively. M_a and N_a

are the memory depth and the nonlinear order of the MP branch, respectively. M_b, M_c and N_b, N_c are memory depths and nonlinearity orders of the lagging and leading branches, respectively. L_b and L_c are the lagging and leading tap lengths, respectively. The generalized memory polynomial model does not separate the nonlinearity and memory effects, and hence all the memory branches use the same high nonlinearity order which results in undesirable high complexity. In order to model a highly nonlinear PA, higher memory depth and nonlinearity order need to be used which increase the model complexity.

2.2.6 Nonuniform Memory Polynomial Model

For the memory polynomial model, equal nonlinearity order is set in all the branches which makes the model bulky especially when used for modeling highly nonlinear power amplifiers with large memory effects. The memory effects in power amplifiers decay with time meaning that the longer time-delayed input signals will not have much effect on the amplifier output. Using this fading property of memory effects, the nonuniform memory polynomial is described in [32] wherein the nonlinearity orders of the different branches are independently identified. This nonuniform memory polynomial model has the form

$$y_{NMP}(n) = \sum_{j=1}^M \sum_{i=1}^{N_j} a_{ji} \cdot x(n+1-j) |x(n+1-j)|^{i-1} \quad (2.14)$$

where N_j represents the nonlinearity order of the j^{th} branch. The first branch has the highest nonlinearity order and for the subsequent branches it is forced to be lower. This model shows good reduction in the coefficients as compared to conventional memory

polynomial model with a comparable performance. The total number of coefficients N_{total} to be determined for this model will be

$$N_{total} = \sum_{j=1}^M N_j \quad (2.15)$$

2.3 Twin Nonlinear Two-Box Models

The twin nonlinear two-box (TNTB) models consist of the LUT or memoryless polynomial function and a memory polynomial [33].

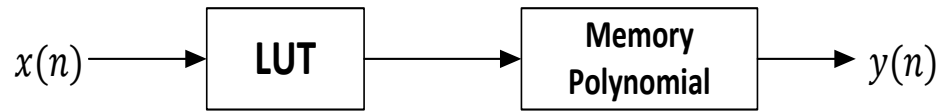


Figure 2.9 Block diagram of the forward TNTB model

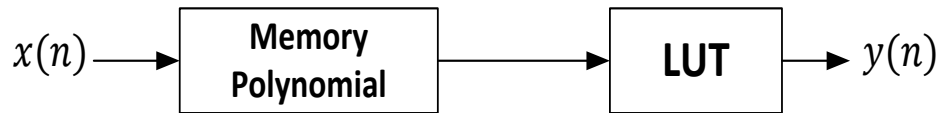


Figure 2.10 Block diagram of the reverse TNTB model

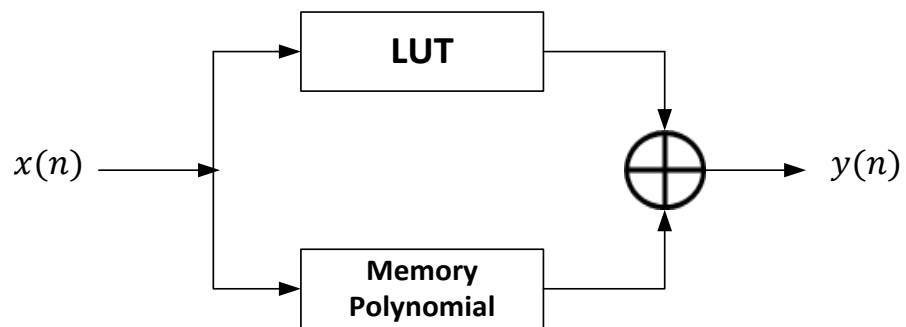


Figure 2.11 Block diagram of the parallel TNTB model

Depending upon the position of LUT and memory polynomial, we have the forward twin nonlinear two-box model (FTNTB) in which the LUT is followed by the memory polynomial function, reverse twin nonlinear two-box model (RTNTB) in which the LUT is placed downstream of the memory polynomial function and parallel twin nonlinear two-box model (PTNTB) in which the LUT and the memory polynomial functions are connected in parallel and the estimated output is the addition of their outputs.

In these two box models, the identification procedure consists of two steps. The highly nonlinear memoryless behavior of DUT is first extracted which corresponds to the LUT box and then the coefficients of the second box which is the MP model are identified. As stated earlier, in the memory polynomial model, each branch has the same high nonlinearity order which in turn leads to more number of coefficients resulting in complexity. For these two-box models the nonlinear static behavior and memory effects are separated which decreases the overall number of parameters by controlling separately the model dimensions. The TNTB models especially the PTNTB was shown to outperform the conventional MP model while reducing the model dimension by upto 50% [33].

2.4 Parallel LUT-MP-EMP Model

The Parallel LUT-MP-EMP (PLUME) model consists of a look-up table, a memory polynomial, and an envelope memory polynomial, all of which are connected in parallel. The outputs of the three models combine to give the output of PLUME [34]. This model does enhance the accuracy of the parallel TNTB model but at the expense of increase in the number of coefficients which can be monitored by proper selection of dimensions of the envelope memory polynomial. PLUME uses limited number of lagging

cross-terms decided by EMP model whereas leading cross-terms are not included. The model dimension estimation is performed in two steps. First the memory polynomial dimensions are evaluated considering PLUME as simply a parallel TNTB. Then EMP model dimensions are identified.

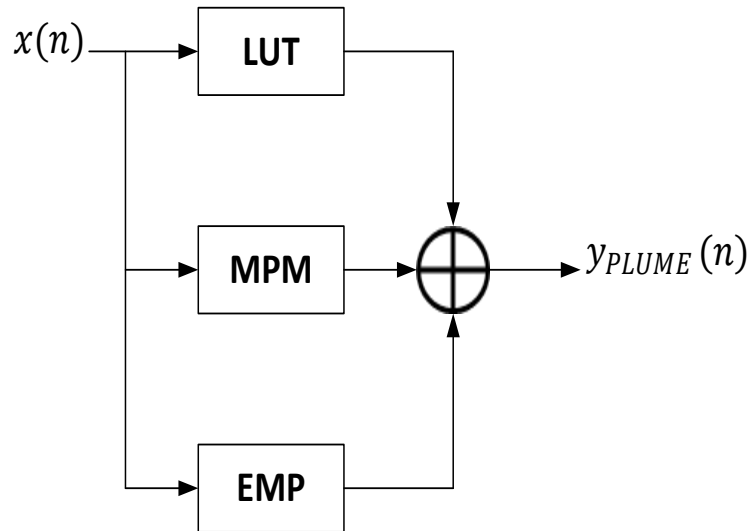


Figure 2.12 Block diagram of the PLUME model

2.5 Generalized TNTB Model

The conventional TNTB model is composed of a memoryless nonlinearity (LUT) and a memory polynomial model whereas in the generalized TNTB model [35] the memoryless look-up table is followed by a generalized memory polynomial function as shown in Figure 2.13 below.

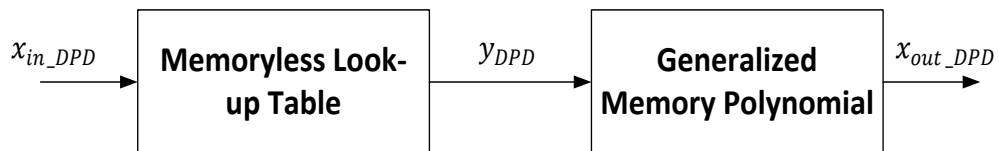


Figure 2.13 Block diagram of the generalized TNTB model

The generalized memory polynomial function is the one given by Equation (2.13). In conventional generalized memory polynomial model, the memory depths and nonlinearity orders are not separated and they are all set equal for the three polynomial functions. Using a 2 box structure makes it possible to reduce the nonlinearity of the polynomial functions used for dynamic distortions. The highly nonlinear static distortion is now represented using polynomial function in the look up table. It has much less number of coefficients as compared to generalized MPM and can be effectively used for modeling nonlinear power amplifiers with strong memory effects.

2.6 Volterra Series Based Models

2.6.1 Volterra Model

Volterra model is used for accurately modeling a dynamic nonlinear system with memory [36] [37]. In discrete time domain, Volterra series formulation is represented as

$$y(n) = \sum_{p=1}^N \sum_{i_1=0}^M \dots \sum_{i_p=0}^M h_p(i_1, \dots, i_p) \prod_{j=1}^p x(n-i_j) \quad (2.16)$$

wherein $x(n)$ and $y(n)$ represent the input and output signals, respectively, and $h_p(i_1, \dots, i_p)$ is called the p th order Volterra kernel. N denotes the nonlinearity order of the model, and M is the memory depth. In this conventional Volterra model all parameters are estimated simultaneously. With increase in the model dimensions, the number of parameters increase drastically which in turn increases the complexity of identifying the coefficients. Therefore, practically it is not possible to use the Volterra model for systems with high nonlinearity order and memory depth. Many of the models described earlier including the two box Wiener and Hammerstein models and the

memory polynomial model are special cases and reduced versions of Volterra series for modeling nonlinear power amplifiers.

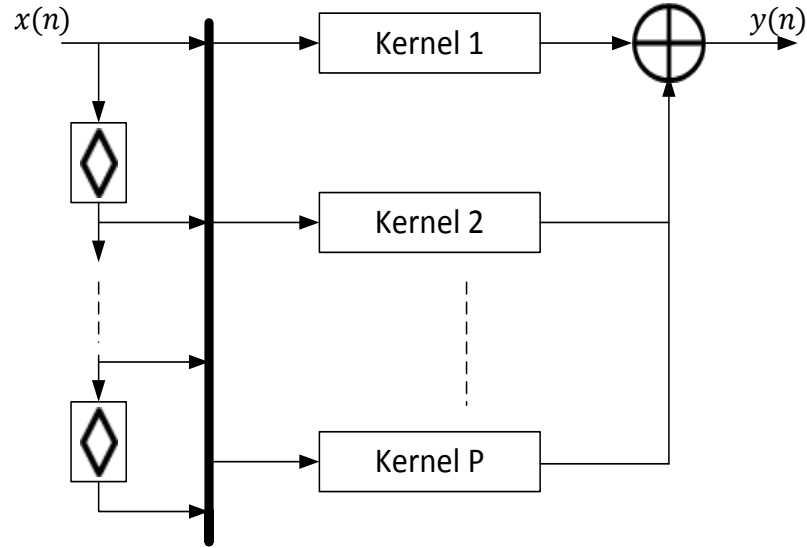


Figure 2.14 Block diagram of the Volterra model

2.6.2 Dynamic Deviation Reduction (DDR) Based Volterra Model

The high complexity of conventional Volterra model is overcome by the modified Volterra series wherein the static nonlinearity and memory effects that are inherently combined in the standard series are separated out. The conventional Volterra representation can be employed only for weakly nonlinear systems as it is difficult to identify the higher order Volterra kernels. This limitation is overcome using a simplified approach proposed in [38] [39] by using the dynamic deviation function $e(n, i)$ which is the difference between the delayed version of input signal $x(n-i)$ and the current input signal $x(n)$.

Thus $e(n, i)$ is given as

$$e(n, i) = x(n-i) - x(n) \quad (2.17)$$

Substituting Equation (2.17) in Equation (2.16), the output $y(n)$ can be expressed as

$$y(n) = y_s(n) + y_d(n) \quad (2.18)$$

where $y_s(n)$ describes the static part of the model and is represented using power series of the present input signal $x(n)$ as

$$y_s(n) = \sum_{p=1}^N a_p x^p(n) \quad (2.19)$$

and the purely dynamic part $y_d(n)$ is a convolution operation with respect to the dynamic deviation $e(n, i)$ and is controlled by the input signal $x(n)$.

$$y_d(n) = \sum_{p=1}^N \sum_{r=1}^p x^{p-r}(n) \sum_{i_1=0}^M \dots \sum_{i_r=0}^M h_{p_r}(i_1, \dots, i_r) \prod_{j=1}^r e(n, i_j) \quad (2.20)$$

Thus, for the first order kernel of this deviation based Volterra series the output $y(n)$ will be

$$y(n) = \sum_{p=1}^N a_p(n) x^p(n) + \sum_{p=1}^N x^{p-1}(n) \sum_{i=1}^M h_{p1}(i) e(n, i) \quad (2.21)$$

As stated earlier, this model is developed by separating and independently estimating the static nonlinearities and dynamic deviation parts. Complex experimental techniques are

required to extract model parameters [38]. Substituting for $e(n,i)$ in Equation (2.21), the output $y(n)$ will be

$$y(n) = \sum_{p=1}^N h_p(n) x^p(n) + \sum_{p=1}^N x^{p-1}(n) \sum_{i=1}^M h_{p1}(i) x(n-i) \quad (2.22)$$

Following the format of Equation (2.22), the general form of the dynamic deviation reduction based Volterra model can be represented as

$$y(n) = \sum_{p=1}^N h_p(n) x^p(n) + \sum_{p=1}^N \left\{ \sum_{r=1}^p \left[x^{p-r}(n) \sum_{i_1=1}^M \dots \sum_{i_r=i_{r-1}}^M h_{p_r}(i_1, \dots, i_r) \prod_{j=1}^r x(n-i_j) \right] \right\} \quad (2.23)$$

The first order deviation based Volterra model in Equation (2.22) is thus the reduction of the general model by selecting $r=1$.

The memory effects in real amplifiers also tend to decay, and as a result the input samples corresponding to high order memory effects have less effect on the output of the amplifier. Moreover, with increasing order, the effect of nonlinearity dynamics is also reduced. It is therefore practical to limit the deviation order to a small value in order to reduce the complexity while at the same time maintaining good accuracy.

The model in Equation (2.23) is thus described as the Deviation Reduction model wherein r denotes the dynamic deviation order. By limiting $1 \leq r \leq 2$ the dynamic parts in Equation (2.23) are reduced to second order and this reduced Volterra model is represented as

$$\begin{aligned}
y(n) = & \sum_{p=1}^N h_p(n)x(n) + \sum_{p=1}^N \left[x^{p-1}(n) \sum_{i=1}^M h_{p1}(i)x(n-i) \right] \\
& + \sum_{p=2}^N \left[x^{p-2}(n) \sum_{i_1=1}^M \sum_{i_2=i_1}^M h_{p2}(i_1, i_2)x(n-i_1)x(n-i_2) \right]
\end{aligned} \tag{2.24}$$

Using this deviation approach, effective tradeoff between the model simplicity and fidelity can be achieved thus allowing Volterra model to be used more in practical applications.

2.6.3 DDR Volterra Model with Fading Memory

Following the work of dynamic deviation based DDR Volterra in [39], a new model is presented in [40] which combines the property of fading memory. In this model, the memory depth is forced to fade with each of the increasing kernel order alongwith eliminating the dynamics of higher order by limiting the deviation order to a small value. The dynamic part $y_d(n)$ in Equation (2.20) is first altered to include only odd orders (h_{p_r}) with $p=\text{odd}$. Secondly, the memory depth for each kernel is independently selected. Starting with a large memory depth M_1 , for the subsequent higher order kernels memory depth is restricted. This is motivated by the fact that deep memory content of the kernels of higher orders do not significantly affect the model performance and reliability. This modified dynamic constituent $y_d(n)$ obtained by independently setting the memory depth M_n for each kernel becomes

$$y_d(n) = \sum_{p=1}^N \sum_{i_1=0}^{M_n} \dots \sum_{i_p=0}^{M_1} h_p(i_1, i_2, \dots, i_p) \prod_{j=1}^p x(n-i_j) \tag{2.25}$$

This model was shown to maintain its fidelity while decreasing the overall number of coefficients as compared to the dynamic deviation based Volterra model [40].

2.7 Complexity Evaluation of PA Behavioral Models

Complexity is an important feature that influences the selection of the behavioral models. The number of coefficients, that are needed to be identified, gives a good indication of the complexity of a behavioral model. This usually depends on the dimensions of the model and it is desirable for the model to achieve high accuracy with less number of coefficients. Table 2.1 describes the complexity of some of the major models in terms of their number of coefficients. With increased model dimensions, and therefore, more complexity, the selected model may be able to achieve high accuracy. However, as mentioned for the Volterra series based models, it is practically not always possible to increase the dimensions beyond a certain limit, as identifying the coefficients becomes difficult. Hence, complexity is an important criterion for comparing and validating the performance of the behavioral models.

In this chapter a thorough review of the different behavioral models has been described. All the above mentioned models are being used for depicting the dynamic nonlinear behavior of PAs. By augmenting the Wiener and Hammerstein models it is possible to account for mild dynamic nonlinearities. The memory polynomial model and its variations are often used for behavioral modeling and digital predistortion applications of power amplifiers that exhibit memory effects. The TNTB models, PLUME model and the generalized TNTB model are able to improve the performance of the memory polynomial based models by separating the static nonlinearity and dynamic distortions. Conventional Volterra model is able to accurately model a dynamic nonlinear system

with memory. However, because of increased complexity it can be used only for modeling weakly nonlinear systems. This drawback is overcome by employing the dynamic deviation reduction based derivatives of the Volterra model.

Table 2.1 Complexity of the different models

Model	Equation	Number of coefficients
Wiener	$x_{out}(n) = f_w[x_1(n)]$ and $x_1(n) = \sum_{j=0}^M h(j) \cdot x_{in}(n-j)$ [23]	$N+M$
Hammerstein	$x_{out}(n) = \sum_{j=0}^M h(j) \cdot x_1(n-j)$ and $x_1(n) = f_H[x_{in}(n)]$ [23]	$N+M$
Memory Polynomial	$y_{MPM}(n) = \sum_{j=1}^M \sum_{i=1}^N a_{ji} \cdot x_{in}(n+1-j) x_{in}(n+1-j) ^{i-1}$ [15]	NM
EMP	$y_{EMPM}(n) = x_{in}(n) \cdot \sum_{j=1}^M \sum_{i=1}^N a_{ji} \cdot x_{in}(n+1-j) ^{i-1}$ [29]	NM
HMEM	$y_{HMEM}(n) = \sum_{j=1}^{M_{MP}} \sum_{i=1}^{N_{MP}} a_{ji} \cdot x(n+1-j) \cdot x(n+1-j) ^{i-1}$ + $\sum_{k=1}^{M_{EMPM}} \sum_{l=1}^{N_{EMPM}} b_{kl} \cdot x(n) \cdot x(n+1-k) ^{l-1}$ [30]	$N_{MPM} \cdot M_{MPM} + N_{EMPM} \cdot M_{EMPM}$
Generalized MP	$y_{GMP}(n) = \sum_{j=1}^{M_a} \sum_{i=1}^{N_a} a_{ji} \cdot x(n+1-j) x(n+1-j) ^{i-1}$ + $\sum_{j=1}^{M_b} \sum_{i=1}^{N_b} \sum_{l=1}^{L_b} b_{jil} \cdot x(n+1-j) x(n+1-j-l) ^{i-1}$ [31] + $\sum_{j=1}^{M_c} \sum_{i=1}^{N_c} \sum_{l=1}^{L_c} c_{jil} \cdot x(n+1-j) x(n+1-j+l) ^{i-1}$	$N_a M_a + N_b M_b L_b + N_c M_c L_c$
Volterra DDR-1	$y(n) = \sum_{i=1}^N h_i(n) x^i(n) + \sum_{i=1}^N x^{i-1}(n) \sum_{j=1}^M h_{i1}(j) x(n-j)$ [39]	$N + NM$
Volterra DDR-2	$y(n) = \sum_{i=1}^N h_i(n) x^i(n) + \sum_{i=1}^N \left[x^{i-1}(n) \sum_{j=1}^M h_{i1}(j) x(n-j) \right]$ + $\sum_{i=2}^N \left[x^{i-2}(n) \sum_{j_1=1}^M \sum_{j_2=j_1}^M h_{p2}(j_1, j_2) x(n-j_1) x(n-j_2) \right]$ [39]	$N+NM + (N-1)M(M+1)/2$

CHAPTER 3

Behavioral Models' Assessment Metrics

An important aspect in behavioral modeling application is selecting an appropriate model that will precisely be able to depict the PA behaviour. Once a model is selected, it is essential to evaluate how accurately it works. Various metrics have been used for validating the accuracy of the behavioral models. Some of these metrics such as normalized mean-square error (NMSE), memory effects ratio (MER) and memory effects modeling ratio (MEMR) are defined in time domain[42]–[44]. Conversely, others namely adjacent channel error power ratio (ACEPR), weighted error-to-signal power ratio (WESPR) and memory effects intensity (MEI) evaluate the model performance in frequency domain considering the power spectrum density of the signals [45]–[47]. Both NMSE and MEMR metrics are largely influenced by the inband error. On the other hand, ACEPR and WESPR are better able to demonstrate the performance of the model in the adjacent channel. All of these metrics are computed by comparing the measured output and the estimated model output.

As shown in Figure 3.1, consider $u_{meas}(n)$ and $y_{meas}(n)$ to be the power amplifier's input and output signals and $y_{model}(n)$ the estimated output using $u_{meas}(n)$ as input. $e(n)$ is the error between measured output and estimated output of model and is given as

$$e(n) = y_{meas}(n) - y_{model}(n) \quad (3.1)$$

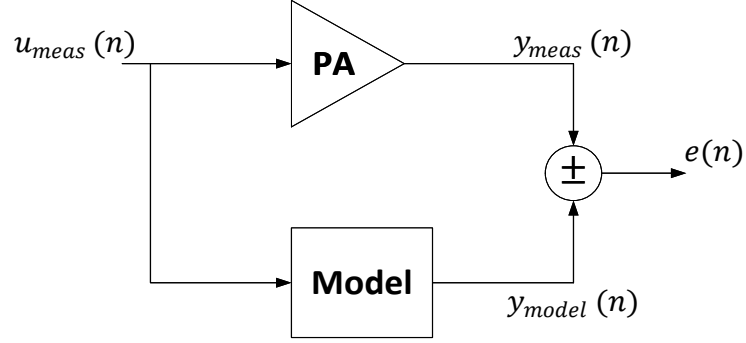


Figure 3.1 Comparison of measured and model output

3.1 Normalized Mean Square Error

The normalized mean square error (NMSE) is given by

$$NMSE = \frac{\sum_{n=1}^N |y_{meas}(n) - y_{model}(n)|^2}{\sum_{n=1}^N |y_{meas}(n)|^2} \quad (3.2)$$

N is the total number of samples of the input and output waveforms. Although NMSE is easy to calculate, it does not reflect accurately the model performance in the adjacent or out-of-band region of the spectrum. It is mainly affected by the in-band error [42].

3.2 Memory Effects Ratio and Memory Effects Modeling Ratio

Memory effects ratio defined in [44] compares the relative level of distortions produced by the DUT due to the presence of memory effects, as compared to the static (memoryless) portion. Memory effects ratio (MER) is defined as the ratio of error produced by the memoryless model to the value of measured output signal as,

$$MER = \frac{\|e^0\|_2}{\|y_{meas}(n)\|_2} = \sqrt{\frac{\sum_{n=1}^N |e^0(n)|^2}{\sum_{n=1}^N |y_{meas}(n)|^2}} \quad (3.3)$$

and

$$e^0 = y_{meas}(n) - y_{model_lut}(n) \quad (3.4)$$

where $y_{meas}(n)$ denotes the measured output and $y_{model_lut}(n)$ is the output of the memoryless LUT model. If the value of the memory effects ratio is large, it indicates that the device has strong memory effect. Using the nonlinear order from memory effects ratio, the memory effects modeling ratio (MEMR) with a length of memory equal to m is

$$MEMR = 1 - \frac{\|e^m\|_2}{\|e^0\|_2} \quad (3.5)$$

and $e^m(n)$ is the error vector defined in Equation (3.1) obtained using a model having a memory depth of m . When all the memory effects in the model are captured this value is 1, and is 0 when memory effects are not considered in the device model [44].

3.3 Adjacent Channel Error Power Ratio and Weighted Error-to-Signal Power Ratio

The adjacent channel error power ratio (ACEPR) and weighted error-to-signal power ratio (WESPR) are better able to detect the model performance in the adjacent channel which corresponds to the out of band error. ACEPR is defined as the error power

in the adjacent channel relative to the power present inside the channel [45] and is calculated as

$$ACEPR = \frac{\int_{adj} |E(f)|^2 df}{\int_{cha} |Y(f)|^2 df} \quad (3.6)$$

where $Y(f)$ and $E(f)$ are the discrete Fourier transforms of $y_{meas}(n)$ and $e(n)$, respectively. $e(n)$ is the error as expressed by Equation (3.1). The channel width and the adjacent channels depend on the signal bandwidth. In [46], the WESPR is defined as,

$$WESPR = \frac{\int_{adj} |W(f)E^m(f)|^2 df}{\int_{cha} |Y_{val}(f)|^2 df} \quad (3.7)$$

where the integration range is as described for ACEPR. The weighting function $W(f)$ is the soft thresholding window calculated as

$$W(f) = \frac{\max \left[\left| E^m(f) \right| \right]}{\max \left[\left| E^m(f) \right| \right] + |U_{meas}(f)|} \quad (3.8)$$

$E^m(f)$ is the Fourier transform of error defined by Equation (3.1) and $U_{meas}(f)$ is the Fourier transform of input $u_{meas}(n)$.

3.4 Memory Effects Intensity

As stated earlier, static nonlinearity is a major factor influencing the overall nonlinearity depicted at the output of a power amplifier whereas the contribution of

memory effects is less. Therefore, while static nonlinearity is present, it is difficult to predict the effect of memory effects on the functioning of a power amplifier. One of the techniques to counter this problem is to apply memoryless digital predistortion [47][48]. However, this method has a key drawback. First, the predistortion function needs to be synthesized and then the PA output signal is measured after applying memoryless predistortion. Moreover, this process is iterative since the analysis of the predistortion function requires more than two sets of measurements. In [19] memoryless post-compensation technique is used for model assessment wherein the static nonlinearity is cancelled at the amplifier's output rather than at its input. Memory effects intensity (MEI) is thus evaluated by calculating the ratio of the spectral powers of the out-of-band spectrum to that of the in-band spectrum after cancelling the memoryless distortion of the DUT [47]. In decibels, the memory effects ratio (MEI) is calculated as,

$$MEI = 10 \log_{10} \left[\frac{\int_{f_c-5B/2}^{f_c-B/2} PSD(f)df + \int_{f_c+B/2}^{f_c+5B/2} PSD(f)df}{\int_{f_c-B/2}^{f_c+B/2} PSD(f)df} \right] \quad (3.9)$$

where f_c denotes the carrier frequency, B represents the bandwidth of the modulated signal and $PSD(f)$ stands for the power spectrum density at frequency f .

3.5 Measurement Set-up

The measurement setup is composed of an arbitrary waveform generator, the device under test (DUT), the vector signal analyzer and a computer to monitor measurements using software as shown in Figure 3.2.

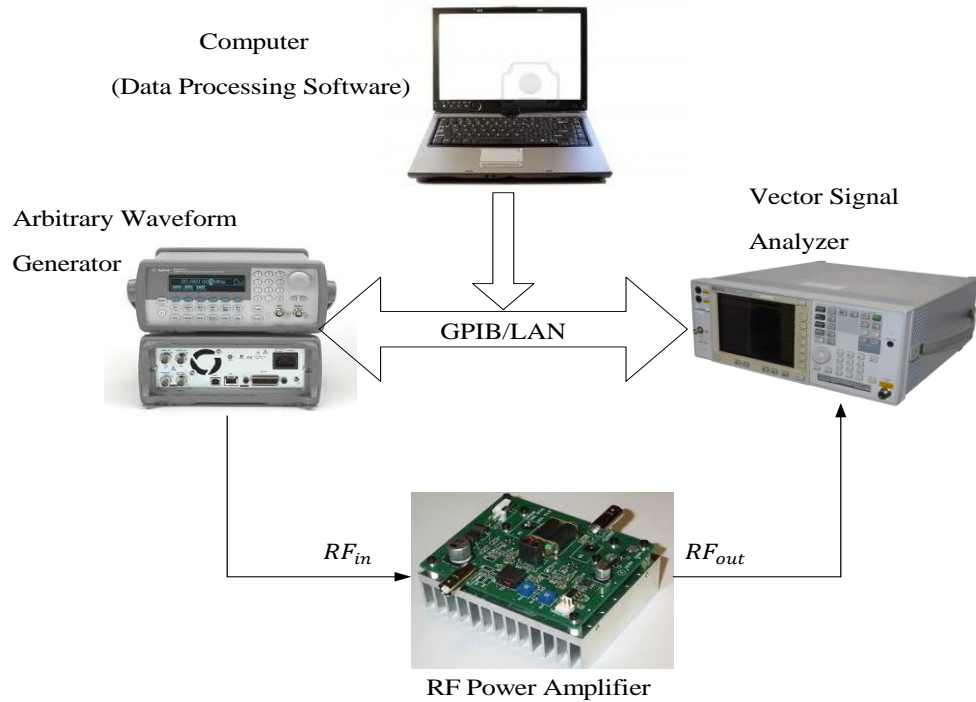


Figure 3.2 Measurement setup for PA characterization

The computer downloads the signal waveform into the arbitrary waveform generator which in turn feeds the DUT with the resultant RF modulated signal. At the DUT output, the measured signal is acquired by the vector signal analyzer that processes the signal and performs signal down conversion and digitization [17]. During the process of obtaining the DUT output there occurs a propagation delay. This propagation delay results in a mismatch between the input and output data samples. If these samples are not aligned, dispersion is observed in the AM/AM and AM/PM characteristics which can be mistaken to be the memory effects exhibited by the DUT. Figure 3.3 shows the AM/AM and AM/PM characteristics using raw measurements and using the time aligned measurements. The input and output signals are therefore, time aligned before generating the behavioural model. The AMPS software is used for time alignment of the signals, the

power adjustment of these waveforms, to generate the FTNTB model and determine the PAPR and the power spectral density of the signals.

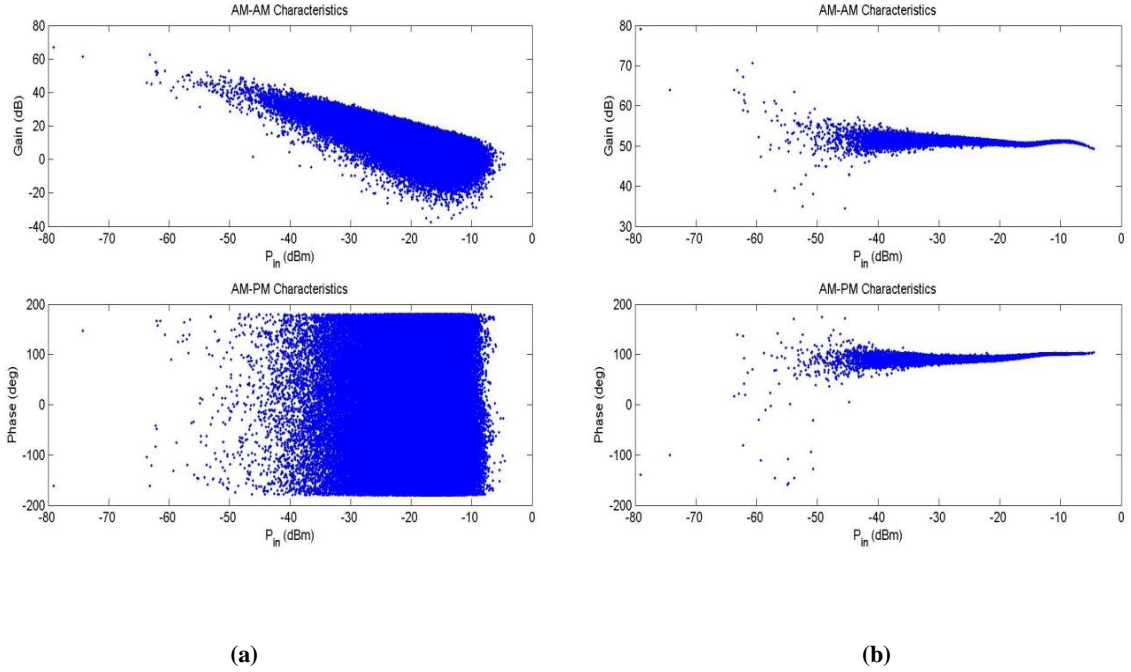


Figure 3.3 AM/AM and AM/PM characteristics of DUT (a) raw data (b) time aligned data

Three different DUTs are used in this work. DUT 1 is a GaN based Doherty operating at 2140MHz. This DUT was tested using a 20MHz LTE signal with PAPR of 11.8 dB and sampled at 92.16MHz. DUT 2 is a class AB PA based on Ericson PTF10107 transistor operating at 1960MHz. Test signal used for this DUT is a 20MHz LTE signal with PAPR of 7.3 dB and sampled at 92.16MHz. DUT 3 is a symmetrical Doherty PA using Cree's 10W packaged GaN devices (CGH400010). The frequency of operation is 2.425GHz. The test signal is a 4-carrier LTE signal with carrier configuration of 1001, in which 0 refers to an OFF carrier and 1 denotes an ON carrier. The bandwidth and PAPR of this signal were 20 MHz and 10 dB, respectively and the signal was sampled at 96 MHz.

Figure 3.4 to Figure 3.6 describe the AM/AM and AM/PM characteristics of the three DUTs.

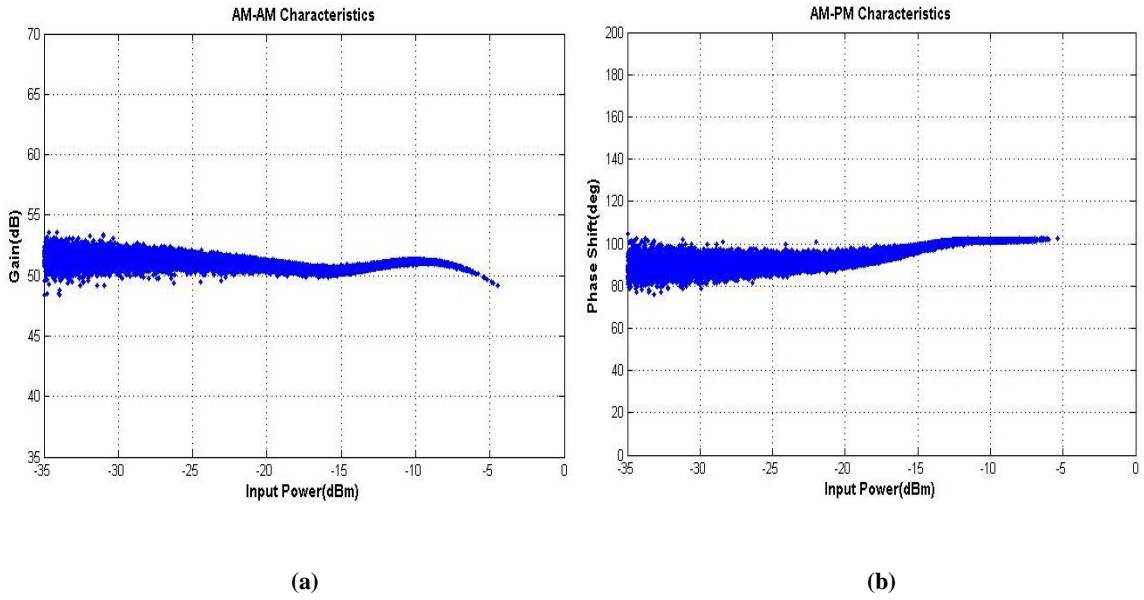


Figure 3.4 DUT 1 characteristics (a) AM/AM characteristics and (b) AM/PM characteristics

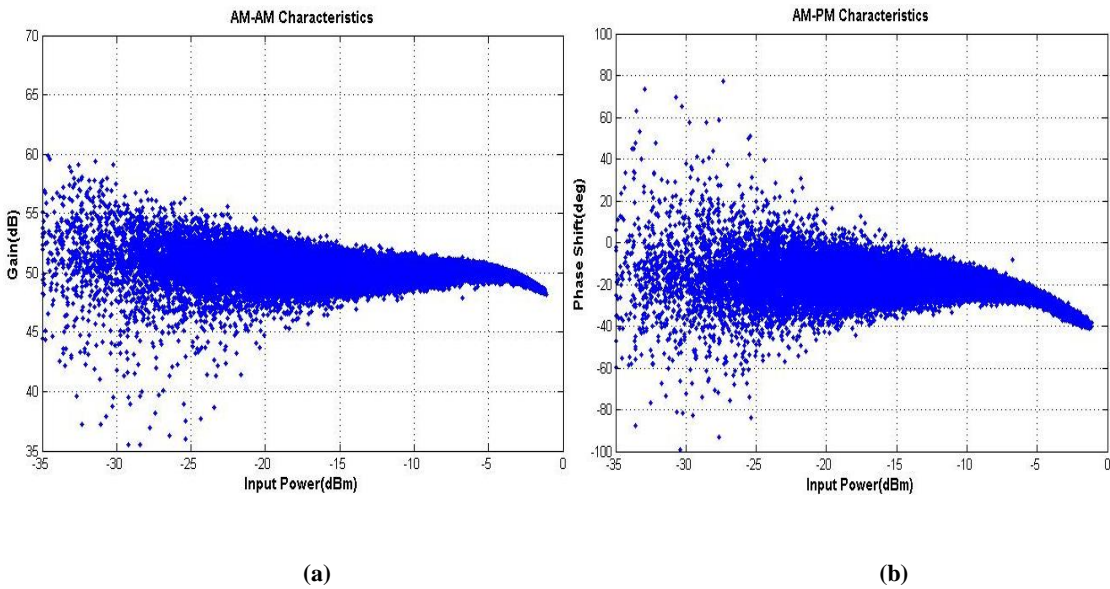


Figure 3.5 DUT 2 characteristics (a) AM/AM characteristics and (b) AM/PM characteristics

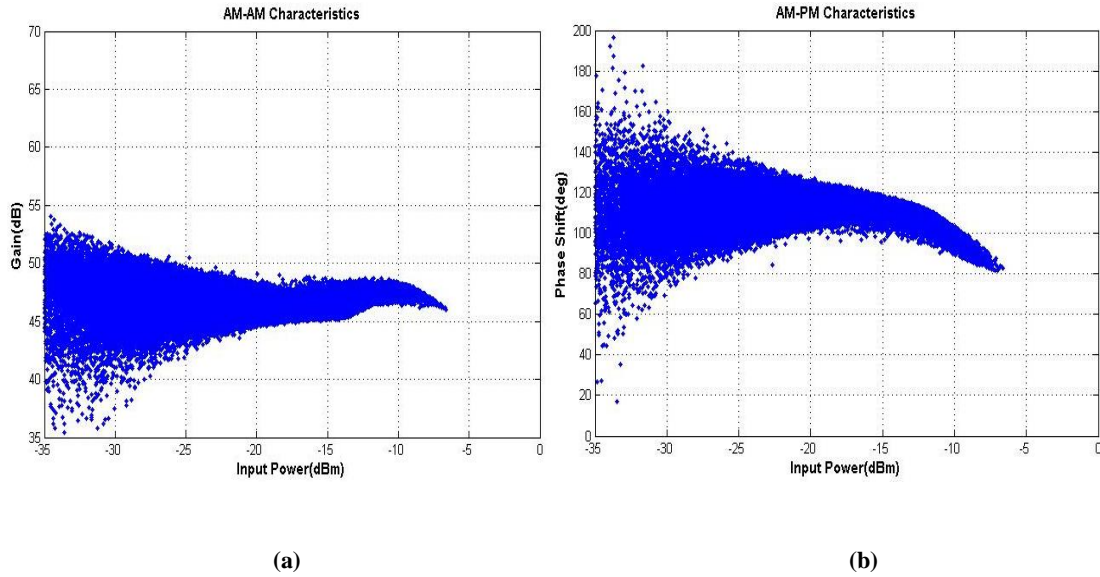


Figure 3.6 DUT 3 characteristics (a) AM/AM characteristics and (b) AM/PM characteristics

3.6 Application of Assessment Metrics for Memory Polynomial Model Dimension Estimation

The parameters of a model determine its size and complexity. The parameters of the memory polynomial model are its nonlinearity order and memory depth. The device under tests' are modelled using the memory polynomial model and its dimensions are determined using various time and frequency domain metrics. The model dimension estimation can be done in two steps for example by first determining the nonlinearity order and then estimating the memory depth.

The input and output files of the DUT are first captured. After doing time alignment, these files are used to extract the memory polynomial model as well as the memoryless post-compensator using AMPS software. Using the software, the signals at the output of the model are estimated. As shown in Figure 3.7, the estimated signals and

the measured signal at the output of the PA are then applied to the memoryless post-compensator and the corresponding post-compensated signals are determined. Comparing the measured and estimated signals, $y_{meas}(n)$ and $y_{model}(n)$, and their post-compensated versions, $y_{meas,postcomp}(n)$ and $y_{model,postcomp}(n)$, the performance assessment metrics are calculated before and after employing post-compensation.

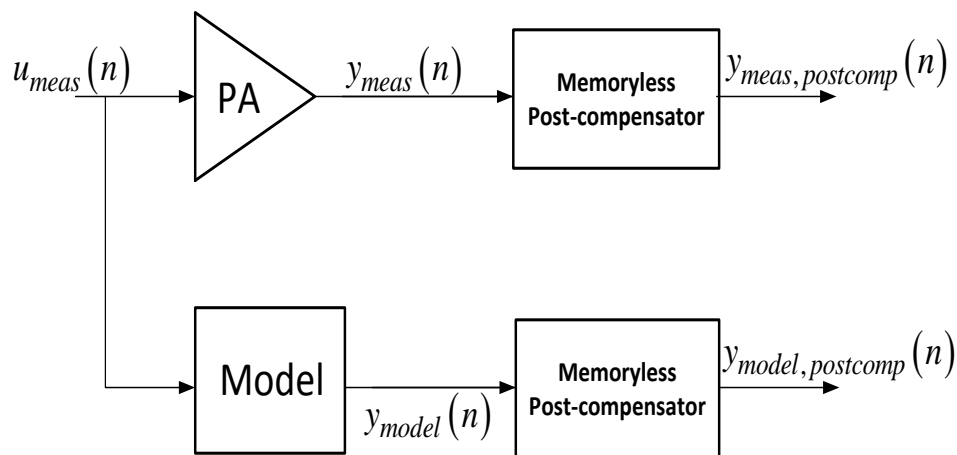


Figure 3.7 Block diagram for the memoryless post-compensation technique

3.6.1 Nonlinearity order estimation

To determine the nonlinearity order, the memory depth of the model is fixed at 0 and the nonlinearity order is varied from 5 to 12. The NMSE, ACEPR and WESPR metrics are calculated for each of the three DUTs and the order which leads to the best values of each of these metrics is noted. N_{NMSE} , N_{ACEPR} and N_{WESPR} are the nonlinearity orders corresponding to the minimum (best) NMSE, ACEPR and WESPR, respectively. For each of the DUTs, the best values of the metrics with their corresponding orders are recorded in Table 3.1 below.

Table 3.1 Model performance of the DUTs

Device Under Test ↓	NMSE		ACEPR		WESPR	
	NMSE value (dB)	Estimated order (N_{NMSE})	ACEPR value (dBm)	Estimated order (N_{ACEPR})	WESPR value (dBm)	Estimated order (N_{WESPR})
DUT 1	-35.4	9	-42.9	9	-57.9	9
DUT 2	-26.5	7	-30.1	7	-50.6	7
DUT 3	-21.9	9	-23.3	9	-40.6	9

As observed from Table 3.1, each of the metrics indicate nonlinearity order of 9 for DUT 1, nonlinearity order of 7 for DUT 2 and nonlinearity order of 9 for DUT 3. Thus, it is observed that all the metrics are consistent and reliable in estimating the nonlinearity order. Once the nonlinearity order is selected the other dimension to be determined is the memory depth.

3.6.2 Memory depth estimation

In order to accurately determine the memory depth, the post-compensation technique is used wherein static nonlinearity is cancelled and the residual distortion left is mainly due to memory effects. Consequently, for each of the DUTs, all the metrics are calculated after post-compensation and the memory depths indicating the best values of the metrics are identified. To determine the memory depth, the MEMR metric is also calculated as it gives a good indication of the presence of memory effects. Using the

nonlinearity order identified in the previous step, the memory depth of the model is varied from 1 to 10 and NMSE, ACEPR, WESPR and MEMR are calculated for each of the DUTs and their values are noted. The memory depths indicated by the metrics for the 3 DUTs before and after post compensation are presented in Table 3.2.

Table 3.2 Memory depth of the DUTs

		NMSE	MEMR	ACEPR	WESPR
DUT 1	Before Post Compensation	1	1	1	1
	After Post Compensation	1	1	1	1
DUT 2	Before Post Compensation	3	2	3	3
	After Post Compensation	3	3	3	3
DUT 3	Before Post Compensation	5	5	3	3
	After Post Compensation	6	6	6	6

The results show that before post-compensation, all the metrics do not indicate the same memory depth of the model as observed for DUT 2 and DUT 3. However, after employing post-compensation, all metrics are consistent and indicate the same memory depth of the model. Table 3.2 indicates that the memory depth for DUT 1, DUT 2 and DUT 3 is 1, 3, and 6, respectively. As observed from Figure 3.4 to Figure 3.6, for DUT 3 there is wide dispersion in the AM/AM and AM/PM characteristics while for DUT 1 the dispersion is much less. Thus, DUT 1 exhibits less memory effects, the memory effects exhibited by DUT 2 are moderate while DUT 3 has strong memory effects.

For each DUT, the memory effects intensity (MEI) values are presented in Table 3.3.

Table 3.3 MEI values of the DUTs

Device Under Test ↓	Memory Effects Intensity	
	Lower Channel	Upper Channel
DUT 1	45.4 dBc	45.7 dBc
DUT 2	40.2 dBc	40.5 dBc
DUT 3	17.7 dBc	21.6 dBc

Higher the MEI value, lower is the memory effect. The MEI value for DUT 1 is high, indicating that it has less memory effects. For DUT 2, MEI is lesser suggesting that it has more memory effects, while among all the three DUTs the MEI value for DUT 3 is the least indicating that it has strong memory effects. Hence, the MEI values further validate the memory depths of 1, 3 and 6 obtained for DUT 1, DUT 2 and DUT 3, respectively as reported in Table 3.2.

3.6.3 Conclusion

In this work, three different power amplifiers have been modelled using the memory polynomial model and its dimensions were determined by evaluating the model performances using the NMSE, MEMR, ACEPR and WESPR metrics. The static nonlinearity order is first identified, and then the memory depth is determined. The post-compensation technique is proved to be a useful method in accurately identifying the memory depth when the device under test has strong memory effects. Thus, with $(N \times M)$ being the size of the memory polynomial model, where N is the nonlinearity order and M is the memory depth, for DUT 1 this size is (9×1) , for DUT 2 the model size is (7×3)

and for DUT 3 the model dimensions are (9x6). The proposed method can be successfully used to determine the accurate size of the memory polynomial model and thus avoid over sizing problems commonly encountered in practice.

CHAPTER 4

Hybrid Twin Nonlinear Two-Box Model

A review of the different behavioral models and their performance evaluation metrics has hitherto been discussed. Because of its relatively simpler structure and accurate performance, the memory polynomial model by itself and in conjunction with some of the other models is extensively used for behavioral modeling of power amplifiers exhibiting memory effects and is often regarded as a benchmark for validating the performance of newly developed models. Moreover, based on the results presented in the previous chapter, the normalized mean square error can be considered a reliable metric for comparing the different models and eventually proposing a behavioral model which is more accurate and has good fidelity in depicting the power amplifier performance. The functioning of these models is largely influenced by the type of power amplifier employed and the characteristics of input and output signals such as their bandwidth, PAPR value, number of carriers, etc. The parameters of a model determine the model size and hence its complexity. Thus, different pruning techniques are being employed to reduce the model size without compromising on accuracy and also to augment the performance with little or no increase in complexity. With this perspective, a modified version of the forward twin nonlinear two-box (FTNTB) model which consists of the look-up table (LUT) model in cascade with the hybrid memory polynomial-envelope memory polynomial (HMEM) model is proposed. Thus, the memory polynomial box in the conventional FTNTB model is replaced by the HMEM structure. The model

performance is validated on Doherty power amplifier driven by wideband LTE-A signals. The model structure and its performance assessment through experimental validation are discussed in the next sections. The experimental set-up for proposed model validation is similar to the one showed in Figure 3.2. The DUT is a 300W Laterally Diffused Metal Oxide Semiconductor (LDMOS) Doherty PA operating at 2140MHz. Two LTE-A signals are used for characterizing the DUT and deriving the behavioural models. The first signal is a 3-carrier 60 MHz signal with carrier configuration of 101, PAPR of 10.8 dB and sampled at 384 MHz. The second signal is an 80MHz signal with carrier configuration of 1001, PAPR of 11.1 dB and sampled at 537 MHz.

4.1 Proposed Hybrid Twin Nonlinear Two-Box (HTNTB) Model

As described in Section 2.3, the TNTB models consist of a look-up table and a memory polynomial arranged in different configurations. The conventional twin nonlinear two-box models outperform the memory polynomial model and provide better accuracy with lesser number of coefficients. In [49], the augmented version of the FTNTB model was proposed as shown in Figure 4.1.

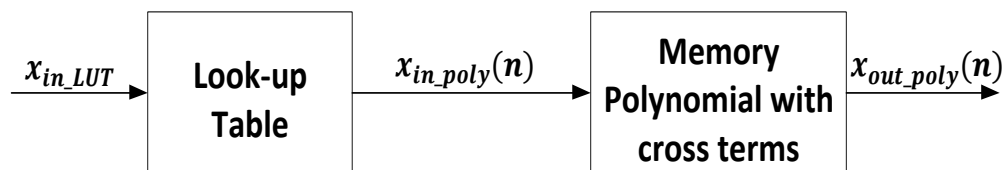


Figure 4.1 Block Diagram of the augmented twin nonlinear two-box model

The memory polynomial function with cross terms is implemented by Equation (2.13). Since there are 8 variables involved, it is computationally complex to determine the

model size by varying each of them. Therefore, the lagging and leading cross-terms L_b and L_c were set equal to 1 [49]. Similarly, the memory depths and nonlinearity orders of the cross-terms were set equal.

$$\begin{aligned}
 M_b &= M_c \\
 N_b &= N_c \\
 L_b &= L_c = 1
 \end{aligned} \tag{4.1}$$

The proposed hybrid twin nonlinear two-box (HTNTB) model is a simplified version of the ATNTB model. Moreover, it is an enhancement of the conventional FTNTB model in which the memory polynomial box is replaced by the HMEM model. The performance of the HTNTB model is compared with that of the FTNTB model and the augmented twin nonlinear two-box (ATNTB) model. This model combines the benefits of both the FTNTB and HMEM model structures and experimental results show that it is able to achieve better modeling performance and accuracy with reduced complexity.

As described in Figure 4.2, in the HTNTB model, the memoryless LUT model is cascaded with the HMEM model which consists of the memory polynomial model and the envelope memory polynomial model connected in parallel. N_{MP} and M_{MP} are the nonlinearity order and memory depth of the memory polynomial model, respectively. N_{EMP} and M_{EMP} are the nonlinearity order and the memory depth of the envelope memory polynomial model, respectively. The performance is assessed in terms of the NMSE metric calculated using the measured output and the output of the proposed model. The LUT model compensates for the highly nonlinear static behaviour which allows for lower nonlinearity order to be used for the MP and EMP models. This significantly reduces the number of coefficients needed for the HMEM model.

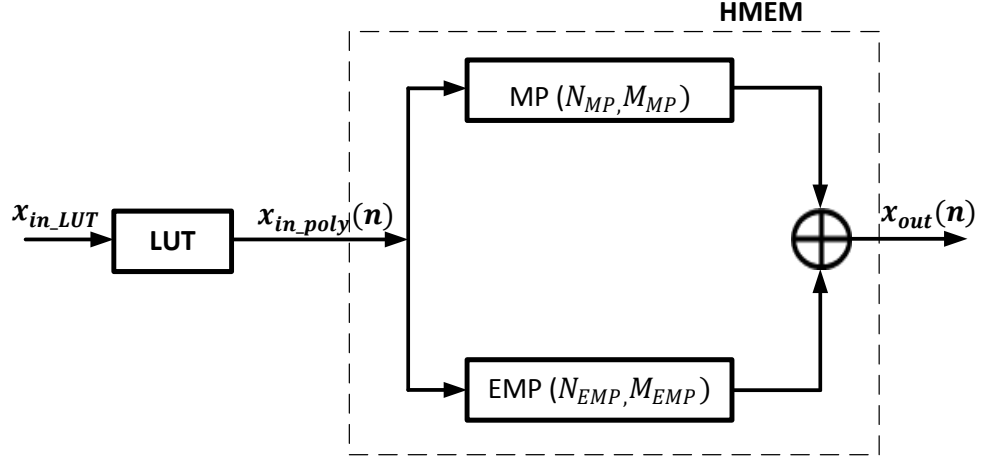


Figure 4.2 Block diagram of the proposed hybrid twin nonlinear two-box model

4.2 Model Identification

In two box model structures, the identification process generally involves two steps. In the first one, the LUT is identified and the input and output signals of the memory polynomial function extracted. In the FTNTB structure, once the LUT is identified, the measured input signal $x_{in}(n)$ of the power amplifier is applied to the LUT model and the polynomial block input signal $x_{in_poly}(n)$ and output signal $x_{out_poly}(n)$ are generated.

$$x_{in}(n) = x_{in_LUT}(n) \quad (4.2)$$

In the next step, using the polynomial box input signal $x_{in_poly}(n)$ and output signal $x_{out_poly}(n)$, the coefficients of the memory polynomial function are identified. These signals are used to identify the polynomial functions of the FTNTB model, the ATNTB

model and the proposed HTNTB model. The output $x_{out}(n)$ of the proposed HTNTB model is given as,

$$x_{out}(n) = x_{out_poly}(n) \quad (4.3)$$

4.2.1 FTNTB model identification

Using the polynomial box input signal $x_{in_poly}(n)$ and output signal $x_{out_poly}(n)$, the memory polynomial model is developed by sweeping the memory depth and nonlinearity order from 1 to 10 each resulting in 100 different sizes of the FTNTB model which is used as a reference. For each of the 100 sizes, the FTNTB model performance is evaluated by calculating NMSE. The results are shown in Figure 4.3. The total number of coefficients for the FTNTB model is given as

$$S_{FTNTB} = N_{LUT} + M_{MP} \cdot N_{MP} \quad (4.4)$$

where S_{FTNTB} is the total number of coefficients of the FTNTB model and, M_{MP} and N_{MP} are the same as those defined in Equation (2.10). N_{LUT} is the size of the polynomial function used to build the LUT. In all the models used in this work, N_{LUT} was set to 10.

With increasing nonlinearity order, the NMSE performance for different values of the memory depths is shown in Figure 4.4. Each curve represents the NMSE performance as a function of the nonlinearity order, for a fixed value of memory depth.

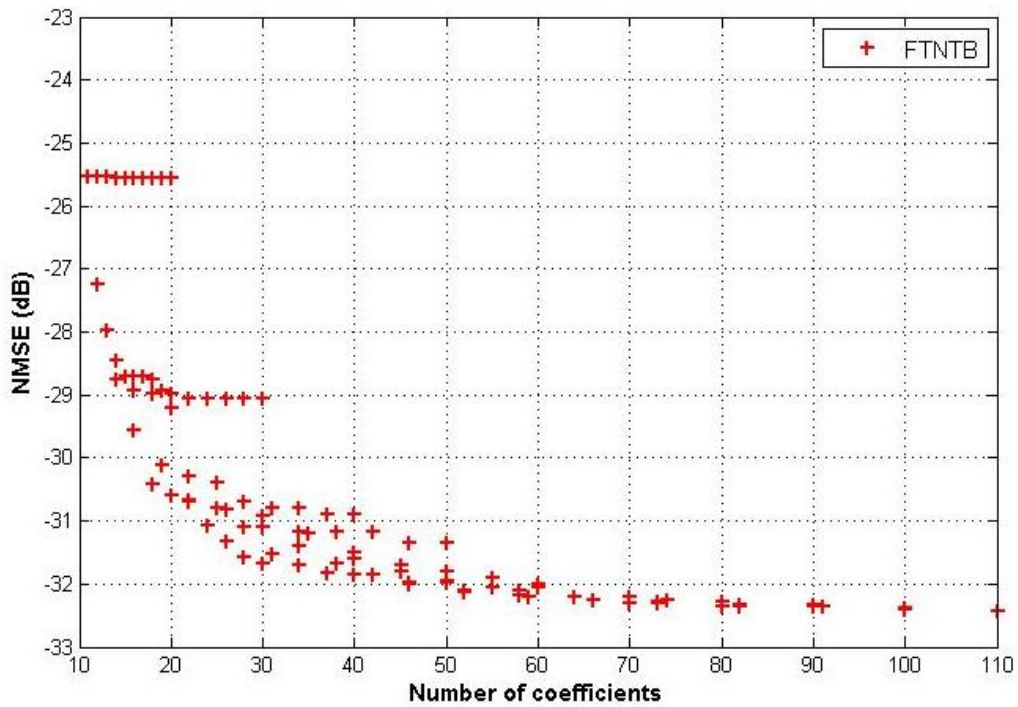


Figure 4.3 FTNTB model performance for the 60MHz LTE-A signal

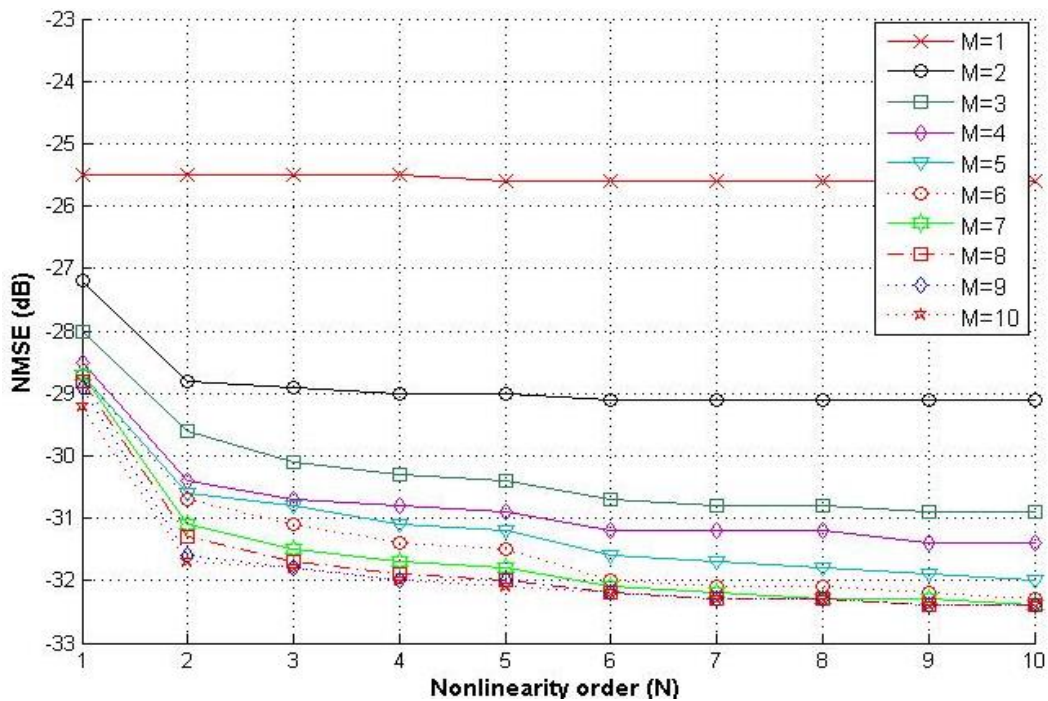


Figure 4.4 FTNTB model performance for 60MHz LTE-A signal as a function of nonlinearity order and memory depth

4.2.2 ATNTB model identification

In the ATNTB model, both the lagging and leading cross-terms L_b and L_c , respectively are set equal to 1. The memory depth M_a and nonlinearity order N_a of the memory polynomial function and the memory depths M_b, M_c and nonlinearity orders N_b, N_c of the lagging and leading cross-terms respectively, are varied from 1 to 10 to develop the memory polynomial function with cross-terms of the ATNTB model. This results in 10,000 different structures of the ATNTB model and the performance of each is assessed in terms of the NMSE metric. The results are summarized in Figure 4.5 which presents the NMSE as a function of the total number of coefficients (S_{ATNTB}). The total number of coefficients S_{ATNTB} for the ATNTB model is given as

$$S_{ATNTB} = N_{LUT} + M_a \cdot N_a + M_b \cdot N_b \cdot L_b + M_c \cdot N_c \cdot L_c \quad (4.5)$$

where all variables are the same as those defined in Equation (2.13)

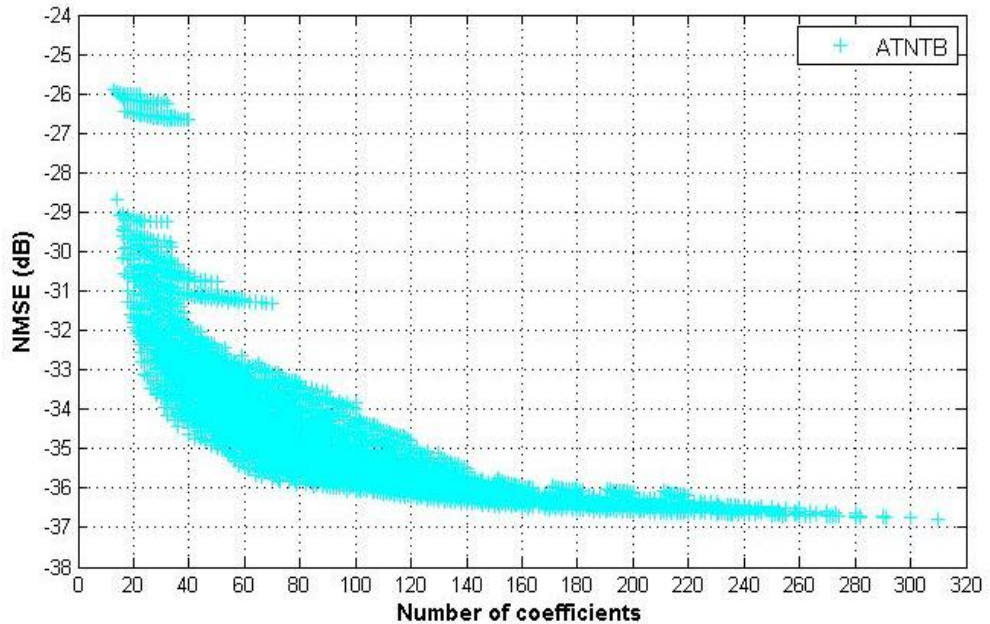


Figure 4.5 ATNTB model performance for the 60MHz LTE-A signal

4.2.3 HTNTB model identification

The HMEM structure of the HTNTB model as described in Figure 4.2 is developed for a wide range of sizes by sweeping the memory depths M_{MP} , M_{EMP} and nonlinearity orders N_{MP} , N_{EMP} of the memory polynomial function and envelope memory polynomial function, respectively from 1 to 10. Similar to the ATNTB model, the sweep of the model dimensions' results in 10,000 different structures of the HTNTB model and their performance was assessed by calculating NMSE. The results are shown in Figure 4.6, which describes the NMSE performance as a function of the total number of coefficients in the model.

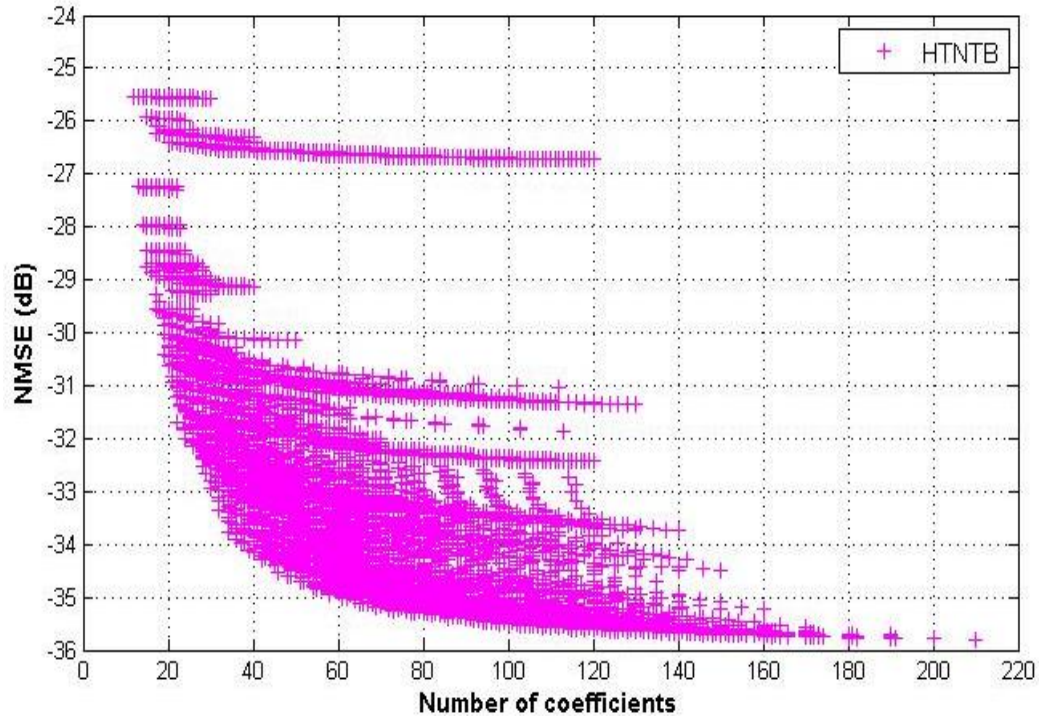


Figure 4.6 HTNTB model performance for the 60MHz LTE-A signal

The total number of coefficients for the HTNTB model is calculated as

$$S_{HTNTB} = N_{LUT} + M_{MP} \cdot N_{MP} + M_{EMP} \cdot N_{EMP} \quad (4.6)$$

where all variables are the same as defined in Equation (2.12) and S_{HTNTB} is the total number of coefficients for the HTNTB model.

In the previous study, the parameters of the FTNTB, ATNTB and HTNTB models were varied over a wide range. For all the resulting model sizes, the NMSE performance is described in Figure 4.3 to Figure 4.6. In these figures, it can be observed that the same number of coefficients can be generated as a result of different combinations of the model parameters, leading to different values of NMSE. In order to have a fair comparison of the performance of the different models based on their best possible performance, Figure 4.7 and Figure 4.8 report the best NMSE as a function of the total number of coefficients for the three considered models for the 60MHz and the 80MHz LTE-A test signals, respectively.

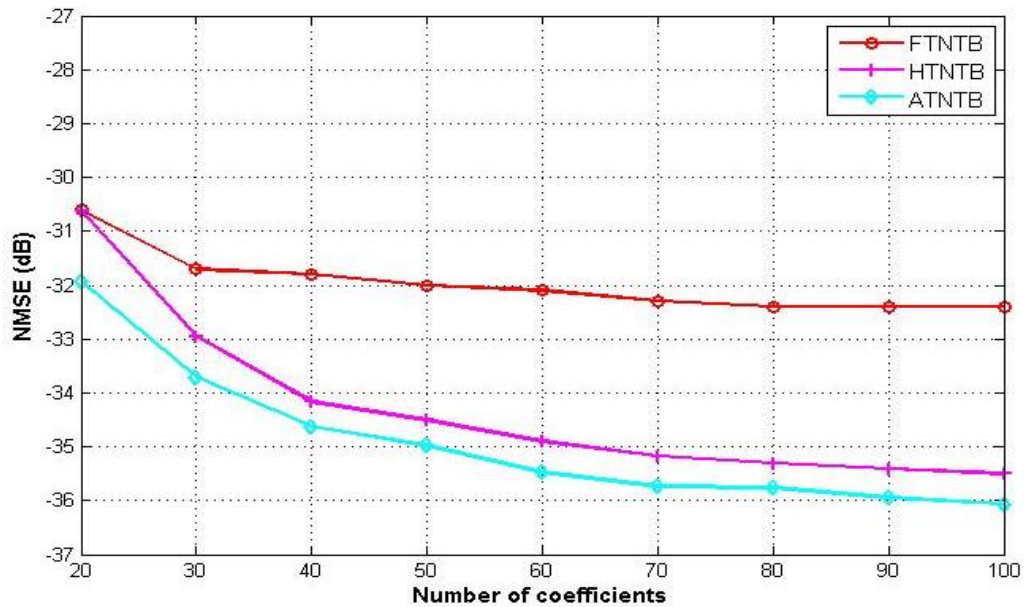


Figure 4.7 NMSE versus number of coefficients for the 60MHz LTE-A signal

Thus, Figure 4.7 and Figure 4.8 show the best NMSE and hence, the best performance of the three two-box structures for the 60MHz and 80MHz LTE-A signals, respectively. Both ATNTB and HTNTB models show good improvement over conventional FTNTB model. As shown in Figure 4.7, for the 60MHz signal, FTNTB model requires 80 coefficients to obtain an NMSE equal to -32.5 dB whereas, with HTNTB and ATNTB models this NMSE is obtained by requiring less than 30 coefficients which is more than 60% reduction in the number of coefficients. And for higher number of coefficients the improvement in NMSE is about 3 dB with the HTNTB model and about 3.5 dB with the ATNTB model.

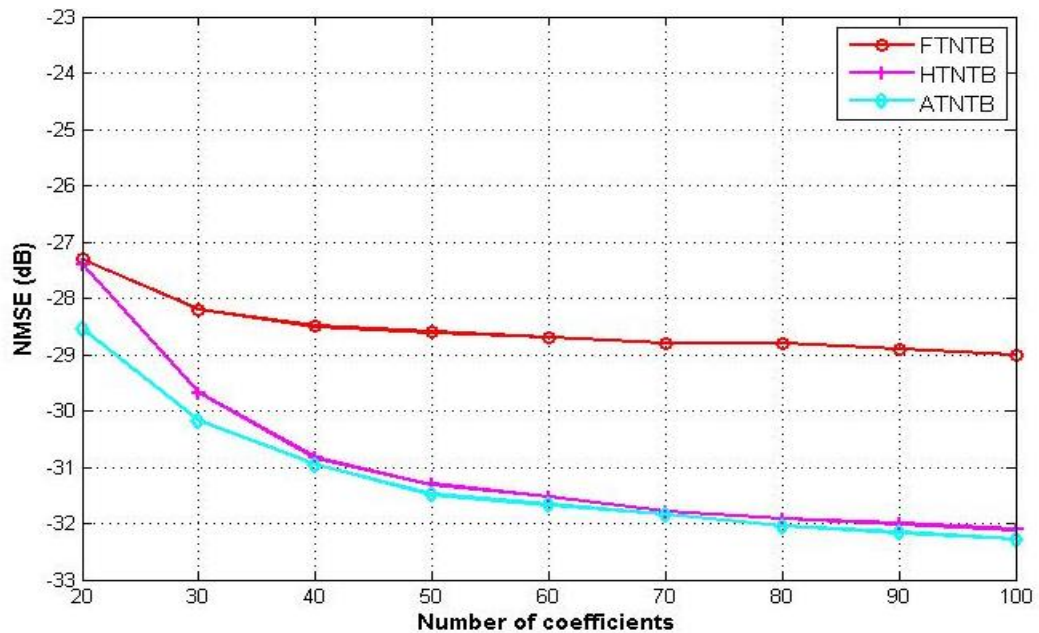


Figure 4.8 NMSE versus number of coefficients for the 80MHz LTE-A signal

A similar result is observed for the 80MHz signal as illustrated in Figure 4.8. The FTNTB model needs more than 90 coefficients to achieve -29 dB NMSE whereas, with

the HTNTB and ATNTB models this NMSE is obtained by requiring less than 30 coefficients which is more than 65% reduction in the number of coefficients. And for higher number of coefficients the improvement in NMSE is about 3 dB with both the modified versions of the FTNTB model.

HTNTB model shows comparable performance with the ATNTB model, particularly when the signal bandwidth increases, but it is relatively less complex because of reduced number of parameters that need to be varied to determine the model's size. The memory polynomial function with cross-terms in ATNTB model structure is determined by eight parameters which make it difficult to tune its size, while only four parameters are necessary for developing the polynomial functions used in the HTNTB model. However, the complexity of the HTNTB model can be significantly reduced by utilising a 2 step approach in determining the two polynomial functions, which is explained in the next section.

4.3 Sequential method for HTNTB model identification

As stated earlier, the HMEM structure in the HTNTB model involves the memory polynomial and envelope memory polynomial models which are defined by 2 parameters each. In Section 4.2.3, the HTNTB model was identified by varying all 4 parameters of the polynomial functions which lead to high computational complexity. Since there are two separate polynomial functions, the complexity can be considerably reduced by first selecting the dimension of one of the polynomial functions and then augmenting it by adding the other polynomial function. This can be done in two ways. By first selecting the memory polynomial function and adding the envelope polynomial function or vice versa. The HMEM identification procedure will thus comprise of two steps.

In Section 3.6.2, it has been studied that, the post-compensation technique is useful for accurately determining the memory depth of the memory polynomial function. However, this technique cannot be applied when there is more than one polynomial function whose memory depth needs to be identified. Since, in Section 4.2.3, the HTNTB model was identified by varying the memory depths and nonlinearity orders of both polynomial functions simultaneously, it is not possible to apply the post-compensation technique. Therefore, in order to have a fair and rational comparison between the HTNTB model identification procedures, the post-compensation technique is not utilized in this sequential identification method.

4.3.1 Augmenting the Memory Polynomial Function

Using the polynomial box input and output signals, the memory polynomial model is developed by sweeping its memory depth and nonlinearity order from 1 to 10. This will result in 100 structures of the memory polynomial model and performance of each is evaluated by NMSE metric.

Using a threshold value of within 0.2dB from the minimum (best) NMSE obtained, the optimum model dimensions are selected having effective trade-off between accuracy and complexity. Once the memory polynomial dimensions are fixed, the memory depth and nonlinearity order of the envelope memory polynomial function are varied from 1 to 10 which results in addition of 100 more model structures. The total number of model structures will thus be equal to 200.

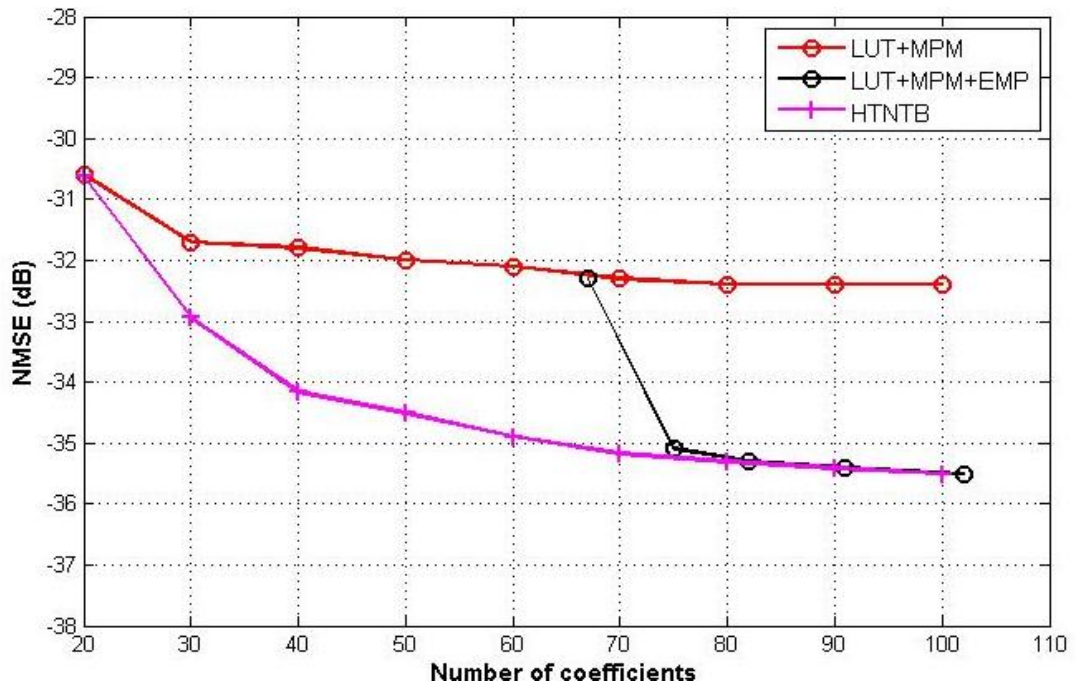
For the 60MHz signal, the memory depth (M_{MP_60}) and the nonlinearity order (N_{MP_60}) are identified as 8 and 7, respectively. Similarly, for the 80MHz signal, the

size of the memory polynomial function is selected as memory depth $(M_{MP_80})=9$ and nonlinearity order $(N_{MP_80})=7$, and it is subsequently augmented by the envelope memory polynomial function. Increase in the memory depth compared to the 60MHz signal is expected because as the bandwidth of the signal increases, the memory effects exhibited by the amplifier tend to increase.

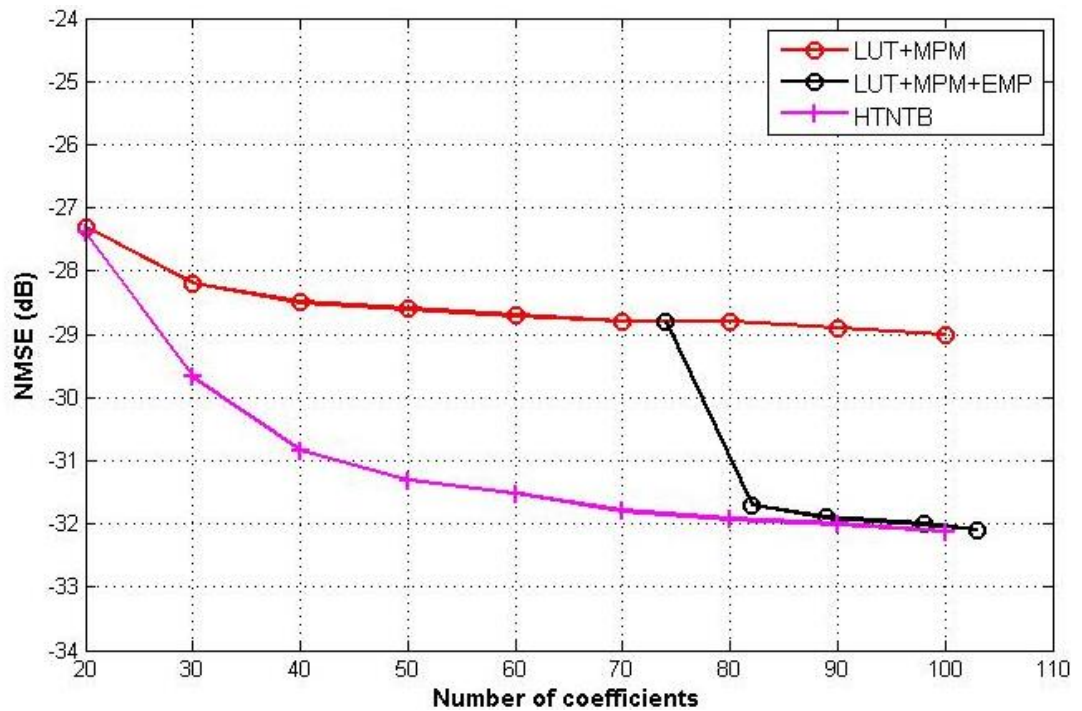
Using this sequential approach, the performance of the HTNTB model, for the 60MHz signal and the 80MHz signal, is shown in Figure 4.9 (a) and Figure 4.9 (b), respectively. In both the figures, the curve labeled LUT+MPM represents the best performance of the FTNTB model. As stated before, once the size of the memory polynomial is fixed, it is augmented by the envelope memory polynomial function and the resulting performance is represented by the curve labeled LUT+MPM+EMP. The curved labeled HTNTB denotes the best performance of the HTNTB model obtained by varying all the four parameters.

For both signals under consideration, it is observed that, by using this sequential approach only 200 structures are needed to converge to the best NMSE performance which was earlier achieved with 10000 structures generated as a result of the concurrent sweep of the polynomial functions' parameters.

Thus, addition of the envelope memory polynomial function helps to improve the performance considerably by increase of a fewer number of coefficients. And this identification procedure helps in reducing the computational complexity as compared to the identification procedure wherein the dimensions of both the polynomial functions are varied simultaneously.



(a)



(b)

Figure 4.9 NMSE performance of the augmented memory polynomial function for (a) 60MHz LTE-A signal and (b) 80MHz LTE-A signal

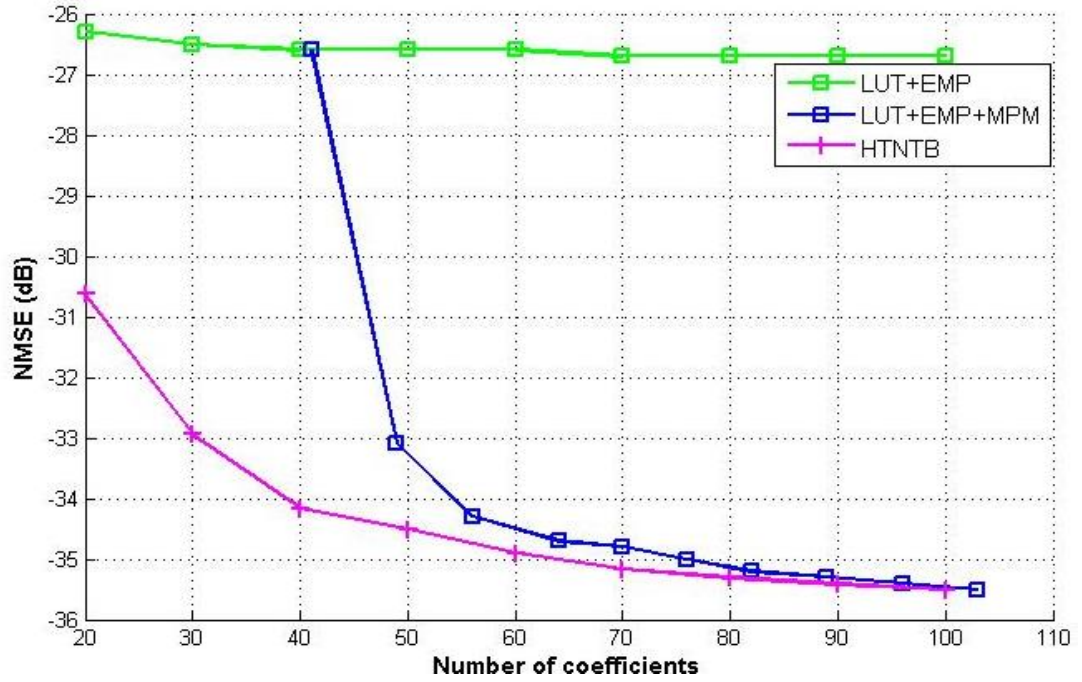
4.3.2 Augmenting the Envelope Memory Polynomial Function

Using a similar approach to the one described in Section 4.3.1, the envelope polynomial dimensions are determined in the first step and subsequently the memory polynomial dimensions are obtained. This subsequent sweep of the envelope polynomial dimensions and the memory polynomial dimensions from 1 to 10 results in 200 model structures.

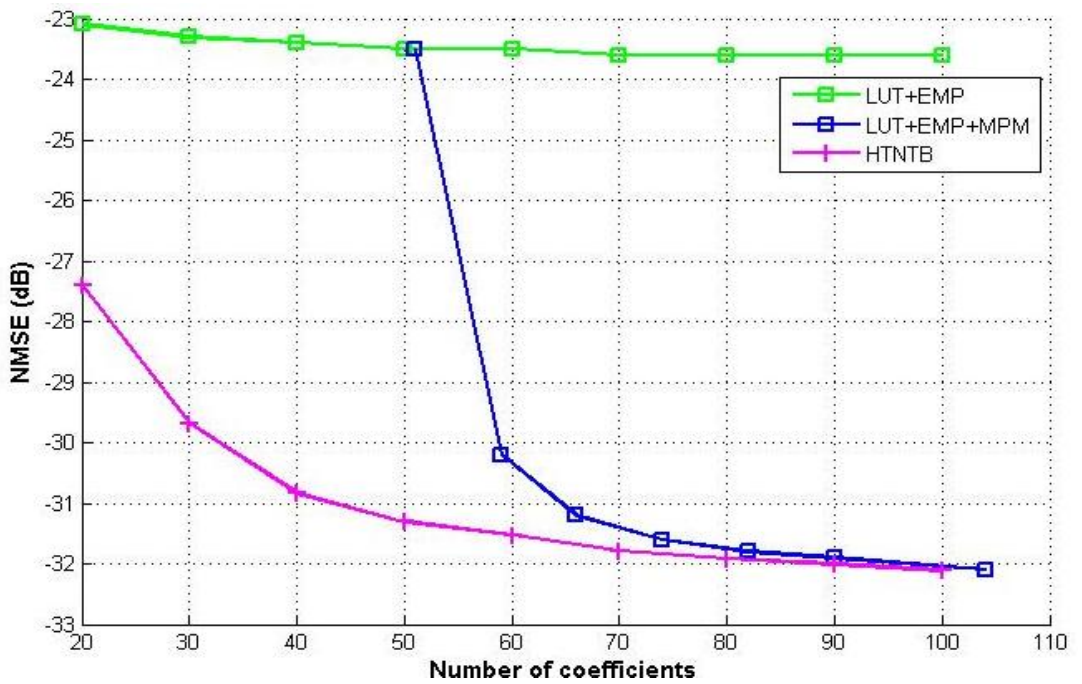
For the 60MHz signal, the memory depth $(M_{EMP_60})=6$ and nonlinearity order $(N_{EMP_60})=5$, and $(M_{EMP_80})=8$ and $(N_{EMP_80})=5$ for the 80MHz signal. Bandwidth of the signal directly affects the memory effects of the amplifier and hence a higher value of memory depth is required for the 80MHz LTE-A test signal as compared to the 60MHz LTE-A signal. The performance of the two signals is reported in Figure 4.10 (a) and Figure 4.10 (b), respectively.

In both the figures, the curve labeled LUT+EMP represents the best performance of the cascade of the look-up table and envelope memory polynomial function. Once the size of the envelope memory polynomial is fixed, it is augmented by the memory polynomial function and the resulting performance is represented by the curve labeled LUT+EMP+MPM. The curve labeled HTNTB denotes the best performance of the HTNTB model obtained by varying all the four parameters.

Similar to the approach in Section 4.3.1, it is observed that, by augmenting the envelope memory polynomial function with the memory polynomial function, only 200 structures are needed to converge to the best NMSE performance of the HTNTB model.



(a)



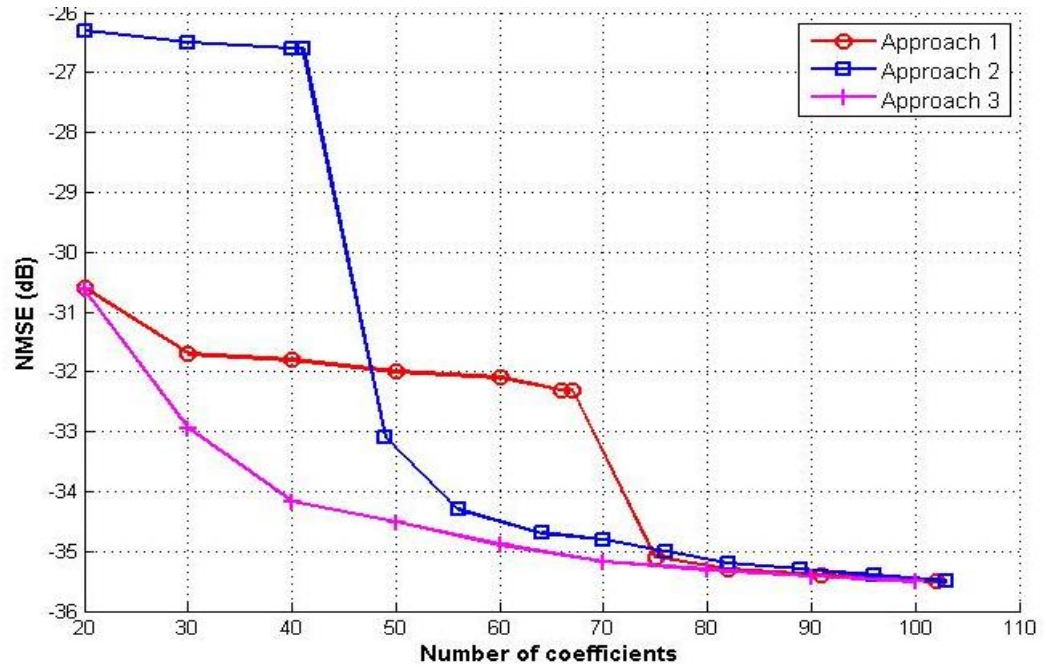
(b)

Figure 4.10 NMSE performance of the augmented envelope memory polynomial function for (a) 60MHz LTE-A signal and (b) 80MHz LTE-A signal

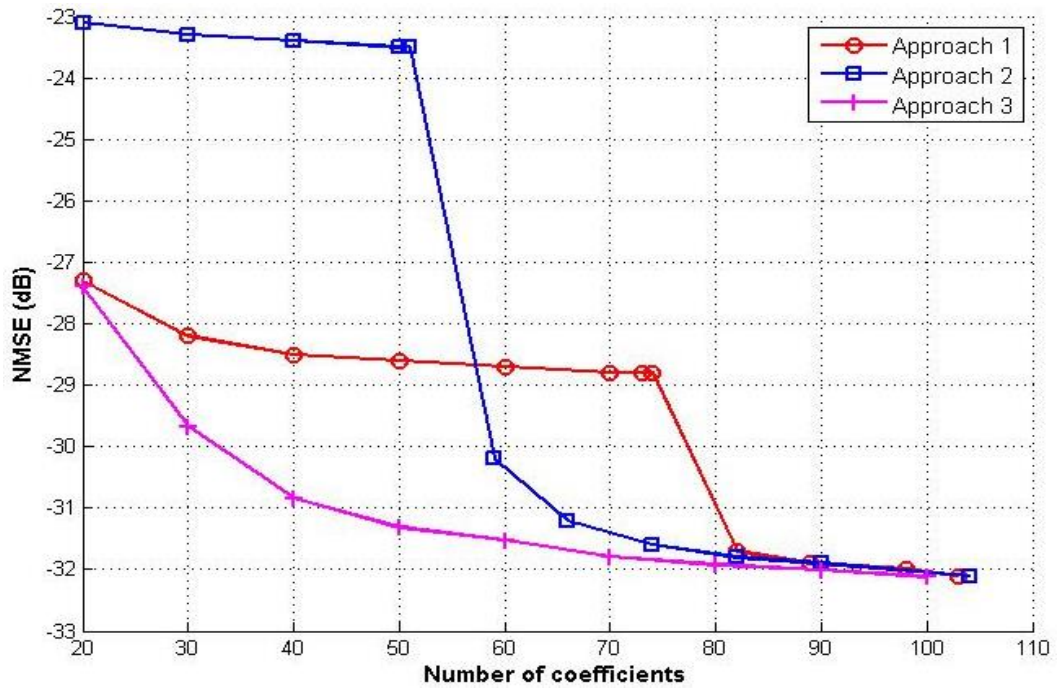
4.4 Comparative Analysis of HTNTB Model Identification

The HTNTB model can thus be identified, by simultaneously varying all the parameters of the polynomial functions and observing the performance, or using one of the sequential identification approaches described in Section 4.3.

Figure 4.11 (a) and Figure 4.11 (b) give a comparative analysis of the different HTNTB model identification approaches for the 60MHz and 80MHz signals, respectively. For both signals, it is observed that, varying all four parameters of the HMEM structure as described in Section 4.2.3, gives better performance especially for a small number of coefficients as compared to the case where the polynomial functions' sizes are identified sequentially. This is represented by the curve labeled Approach 3. However, the computational complexity associated with the simultaneous variation of all four parameters of the HMEM sub-model is high as it involves 10,000 different combinations of the model dimensions. Besides, it requires a lot of simulation time. Identifying the HMEM model dimensions can be made simpler by using a two-step sequential approach thereby achieving effective trade-off between complexity and performance. Since the memory polynomial (MP) model and the envelope memory polynomial (EMP) model by themselves are well established polynomial based models, identifying their dimensions one at a time is found effective in reducing the computational complexity of identifying the HMEM model size by about 98%. The amount of simulation time also reduces considerably. Approach 1 represents the method where the memory polynomial function is augmented by the envelope memory polynomial function and in Approach 2 the envelope memory polynomial function is augmented by the memory polynomial function as described in Section 4.3.



(a)



(b)

Figure 4.11 Comparative Analysis of HTNTB Model Identification for (a) 60MHz signal and (b) 80MHz LTE-A signal

For both signals under consideration, it is observed that identifying the envelope polynomial dimensions first converges faster, however it has poor initial performance. Identifying the memory polynomial function first converges slower but it has good initial performance even for lesser number of coefficients. For both the 60MHz and 80MHz signals, 3dB improvement over the conventional FTNTB model is achieved with the proposed model. As the model size and number of coefficients increases, the performance of the models obtained with the three identification procedures becomes equivalent. However, it is preferable to use the sequential approaches of identifying the HMEM structure of the HTNTB model because of reduced complexity.

CHAPTER 5

Conclusion and Future Work

The objective of this work was to propose a new behavioural model that will accurately depict the performance of a power amplifier driven by LTE-advanced signals. The LTE-advanced signals are characterized by wide bandwidths upto 100MHz and high PAPR. In order to understand about behavioural modeling and their applications a thorough review of PA behavioural models was presented. A study of metrics used for evaluating their performance was carried out and used to identify reliable model performance assessment metrics. Using GaN based Doherty amplifiers and a class AB PA driven by 20MHz single and multicarrier signals, the metrics were evaluated to help identify the dimensions of the memory polynomial model which is commonly used for depicting the nonlinear behaviour of a power amplifier. The memoryless post-compensation technique was found useful for accurately identifying the memory depth. The proposed identification method was successfully used to determine the accurate size of the memory polynomial model and thus avoid over sizing problems commonly encountered in practice.

A new hybrid twin nonlinear two-box (HTNTB) model built on the FTNTB model structure was proposed. In this model, the memory polynomial box of the conventional FTNTB model was replaced by the HMEM model. A 300W LDMOS Doherty PA driven by LTE-A wideband signals was used for model performance validation. The conventional FTNTB model structure improves the modeling accuracy of

the memory polynomial model whereas the HMEM model gives better modeling performance when the amplifier is driven by wideband signals, especially the signals having OFDM carriers. The proposed HTNTB model thus combines the advantages of both the FTNTB and HMEM models and provides better performance with reduced complexity. For the 60MHz LTE-A signal, best NMSE of about -32.5 dB is achieved with 80 coefficients using the conventional FTNTB model after which the model performance saturates and further increase in model size does not lead to any significant improvement in performance. A similar result is observed for the 80MHz LTE-A signal. However, with the HTNTB model, there is a continuous improvement in model performance with increase in model size. With the proposed HTNTB model upto 3 dB NMSE improvement is obtained for the 60MHz LTE-A signal and more than 3 dB improvement for the 80MHz LTE-A signal. Furthermore, for obtaining the same NMSE performance, the HTNTB model requires 60% less coefficients. Moreover, The HTNTB model gives comparable performance as that of the ATNTB model and at the same time has lesser complexity because only four parameters are varying as opposed to eight in the case of the ATNTB model.

Using the sequential approach for identifying the HMEM structure of the HTNTB model makes it possible to reduce the computational complexity and simulation time involved in the two-step identification approach. With the typical two-step identification approach, the parameters of both the polynomial functions used in the HMEM model have to be varied simultaneously over a wide range of sizes which in turn increases the computational complexity. If, however, the polynomial functions of the HMEM model

are identified one by one in succession, this reduced the computational complexity by 98% in our tests.

The sequential approach proposed for identifying the size of the hybrid memory polynomial function of the HTNTB model can be extended to the case of the generalized memory polynomial. Accordingly, the complexity of the augmented version of the twin nonlinear two-box model can be reduced by employing the sequential approach of identifying the memory depths and nonlinearity orders of the polynomial function and the lagging and leading cross-terms. Once the optimum dimensions of the memory polynomial function are identified, the lagging and leading cross-terms can be added, either together or one after another. This sequential identification will allow for more accurate memory depths and nonlinearity orders to be used for the cross-terms which in turn will reduce the number of coefficients and computational complexity associated with the ATNTB model.

Furthermore, the scope of this work can be extended to digital predistortion in order to compensate for the distortions of power amplifiers driven by LTE-A signals. Based on the results achieved in behavioral modeling context, it is expected that building the predistortion function using the HTNTB model will outperform conventional predistorters. The proposed HTNTB behavioural model can be utilized for digital predistortion application using the RTNTB structure.

This thesis work focused on a single frequency band in which the multi-carrier LTE-A signal is located. However, there is a growing number of LTE frequency bands assigned for possible use with LTE. LTE-Advanced needs bandwidth of upto 100 MHz

and therefore channel aggregation over a wide range of frequencies spanning over more than one frequency band may be needed. The work presented in this thesis can be extended to the case of multiple-band LTE-A systems.

References

- [1] S. Abeta, "Toward LTE commercial launch and future plan for LTE enhancements (LTE-Advanced)," in *2010 IEEE International Conference on Communication Systems*, pp. 146–150, Nov. 2010.
- [2] S. Parkvall, E. Dahlman, A. Furuskar, Y. Jading, M. Olsson, S. Wanstedt, and K. Zangi, "LTE-Advanced - Evolving LTE towards IMT-Advanced," in *2008 IEEE 68th Vehicular Technology Conference*, pp. 1–5, Sept. 2008.
- [3] A. Ghosh, R. Ratasuk, B. Mondal, N. Mangalvedhe, and T. Thomas, "LTE-advanced: next-generation wireless broadband technology [Invited Paper]," *IEEE Wirel. Commun.*, vol. 17, no. 3, pp. 10–22, June 2010.
- [4] R. Ratasuk, D. Tolli, and A. Ghosh, "Carrier aggregation in LTE-Advanced," in *2010 IEEE 71st Vehicular Technology Conference*, pp. 1–5, May 2010.
- [5] M. A. M. Al-Shibly, M. H. Habaebi, and J. Chebil, "Carrier aggregation in Long Term Evolution-Advanced," in *2012 IEEE Control and System Graduate Research Colloquium*, pp. 154–159, July 2012.
- [6] "LTE Advanced Carrier Aggregation | Qualcomm." [Online]. Available: <http://www.qualcomm.com/solutions/wireless-networks/technologies/carrier-aggregation>. [Accessed: 16-Mar-2014].
- [7] Global mobile Suppliers Association, "Evolution to LTE Report," 2014.
- [8] C. E. Weitzel, "RF power amplifiers for wireless communications," in *24th Annual Technical Digest Gallium Arsenide Integrated Circuit (GaAs IC) Symposium*, pp. 127–130, Oct. 2002.
- [9] Y. Y. Woo, Y. Yang, J. Yi, J. Nam, J. H. Cha, and B. Kim, "Feedforward amplifier for WCDMA base stations with a new adaptive control method," in *2002 IEEE MTT-S International Microwave Symposium Digest*, vol. 2, pp. 769–772, June 2002.
- [10] E. E. Eid, F. M. Ghannouchi, and F. Beaugard, "Optimal feedforward linearization system design.," *Microw. J.*, Nov. 1995.
- [11] Y. Kim, Y. Yang, S. Kang, and B. Kim, "Linearization of 1.85 GHz amplifier using feedback predistortion loop," in *1998 IEEE MTT-S International Microwave Symposium Digest*, vol. 3, pp. 1675–1678, June 1998.

- [12] H.-H. Chen, C.-H. Lin, P.-C. Huang, and J.-T. Chen, "Joint polynomial and look-up-table predistortion power amplifier linearization," *IEEE Trans. Circuits Syst. II Express Briefs*, vol. 53, no. 8, pp. 612–616, Aug. 2006.
- [13] A. Zhu, and T. J. Brazil, "An adaptive Volterra predistorter for the linearization of RF high power amplifiers," in *2002 IEEE MTT-S International Microwave Symposium Digest*, vol. 1, pp. 461–464, June 2002.
- [14] N. Safari, T. Roste, P. Fedorenko, and J. S. Kenney, "An approximation of Volterra series using delay envelopes, applied to digital predistortion of RF power amplifiers with memory effects," *IEEE Microw. Wirel. Components Lett.*, vol. 18, no. 2, pp. 115–117, Feb. 2008.
- [15] J. Kim, and K. Konstantinou, "Digital predistortion of wideband signals based on power amplifier model with memory," *Electron. Lett.*, vol. 37, no. 23, p. 1417, Nov. 2001.
- [16] "RF Power Amplifier Behavioral Modeling :: RF and Microwave Engineering :: Cambridge University Press." [Online]. Available: <http://www.cambridge.org/ve/academic/subjects/engineering/rf-and-microwave-engineering/rf-power-amplifier-behavioral-modeling>. [Accessed: 19-Mar-2014].
- [17] F. M. Ghannouchi, and O. Hammi, "Behavioral modeling and predistortion," *IEEE Microw. Mag.*, vol. 10, no. 7, pp. 52–64, Dec. 2009.
- [18] O. Hammi, S. Carichner, B. Vassilakis, and F. M. Ghannouchi, "Synergetic crest factor reduction and baseband digital predistortion for adaptive 3G Doherty power amplifier linearizer design," *IEEE Trans. Microw. Theory Tech.*, vol. 56, no. 11, pp. 2602–2608, Nov. 2008.
- [19] O. Hammi, S. Carichner, B. Vassilakis, and F. M. Ghannouchi, "Power amplifiers' model assessment and memory effects intensity quantification using memoryless post-compensation technique," *IEEE Trans. Microw. Theory Tech.*, vol. 56, no. 12, pp. 3170–3179, Dec. 2008.
- [20] J. K. Cavers, "Amplifier linearization using a digital predistorter with fast adaptation and low memory requirements," *IEEE Trans. Veh. Technol.*, vol. 39, no. 4, pp. 374–382, Nov. 1990.
- [21] Y. Nagata, "Linear amplification technique for digital mobile communications," in *IEEE 39th Vehicular Technology Conference*, pp. 159–164, May 1989.
- [22] M. Schetzen, "Nonlinear system modeling based on the Wiener theory," *Proc. IEEE*, vol. 69, no. 12, pp. 1557–1573, Dec. 1981.

- [23] P. L. Gilabert, G. Montoro, and E. Bertran, "On the Wiener and Hammerstein models for power amplifier predistortion," in *2005 Asia-Pacific Microwave Conference Proceedings*, vol. 2, pp. 1–4, Dec. 2005.
- [24] L. Ding, R. Raich, and G. T. Zhou, "A Hammerstein predistortion linearization design based on the indirect learning architecture," in *IEEE International Conference on Acoustics Speech and Signal Processing*, vol. 3, pp. 2689–2692, May 2002.
- [25] S. Boumaiza, and F. M. Ghannouchi, "Deembedding static nonlinearities and accurately identifying and modeling memory effects in wide-band RF transmitters," *IEEE Trans. Microw. Theory Tech.*, vol. 53, no. 11, pp. 3578–3587, Nov. 2005.
- [26] S. Boumaiza, and F. M. Ghannouchi, "Augmented Hammerstein predistorter for linearization of broad-band wireless transmitters," *IEEE Trans. Microw. Theory Tech.*, vol. 54, no. 4, pp. 1340–1349, Jun. 2006.
- [27] L. Ding, S. Member, G. T. Zhou, S. Member, D. R. Morgan, Z. Ma, J. S. Kenney, J. Kim, and C. R. Giardina, "A robust digital baseband predistorter constructed using memory polynomials," *IEEE Trans. Commun.*, vol. 52, no. 1, pp. 159–165, Jan. 2004.
- [28] R. Raich, H. Qian, and G. T. Zhou, "Orthogonal polynomials for power amplifier modeling and predistorter design," *IEEE Trans. Veh. Technol.*, vol. 53, no. 5, pp. 1468–1479, Sept. 2004.
- [29] O. Hammi, F. M. Ghannouchi, and B. Vassilakis, "A compact envelope-memory polynomial for RF transmitters modeling with application to baseband and RF-digital predistortion," *IEEE Microw. Wirel. Components Lett.*, vol. 18, no. 5, pp. 359–361, May 2008.
- [30] O. Hammi, M. Younes, and F. M. Ghannouchi, "Metrics and methods for benchmarking of RF transmitter behavioral models with application to the development of a hybrid memory polynomial Model," *IEEE Trans. Broadcast.*, vol. 56, no. 3, pp. 350–357, Sept. 2010.
- [31] D. R. Morgan, Z. Ma, J. Kim, M. G. Zierdt, and J. Pastalan, "A generalized memory polynomial model for digital predistortion of RF power amplifiers," *IEEE Trans. Signal Process.*, vol. 54, no. 10, pp. 3852–3860, Oct. 2006.
- [32] O. Hammi, A. M. Kedir, and F. M. Ghannouchi, "Nonuniform memory polynomial behavioral model for wireless transmitters and power amplifiers," in *2012 Asia Pacific Microwave Conference Proceedings*, pp. 836–838, Dec. 2012.

- [33] O. Hammi and F. M. Ghannouchi, "Twin nonlinear two-box models for power amplifiers and transmitters exhibiting memory effects with application to digital predistortion," *IEEE Microw. Wirel. Components Lett.*, vol. 19, no. 8, pp. 530–532, Aug. 2009.
- [34] M. Younes, O. Hammi, A. Kwan, and F. M. Ghannouchi, "An Accurate Complexity-Reduced 'PLUME' Model for Behavioral Modeling and Digital Predistortion of RF Power Amplifiers," *IEEE Trans. Ind. Electron.*, vol. 58, no. 4, pp. 1397–1405, Apr. 2011.
- [35] O. Hammi, M. S. Sharawi, and F. M. Ghannouchi, "Generalized twin-nonlinear two-box digital predistorter for GaN based LTE Doherty power amplifiers with strong memory effects," in *2013 IEEE International Wireless Symposium (IWS)*, pp. 1–4, Apr. 2013.
- [36] M. Schetzen, "*The Volterra and Wiener theories of nonlinear systems*," Apr. 1980.
- [37] A. Zhu and T. J. Brazil, "An overview of Volterra series based behavioral modeling of RF/Microwave power amplifiers," in *2006 IEEE Annual Wireless and Microwave Technology Conference*, pp. 1–5, Dec. 2006.
- [38] D. Mirri, G. Luculano, F. Filicori, G. Pasini, G. Vannini, and G. P. Gabriella, "A modified Volterra series approach for nonlinear dynamic systems modeling," *IEEE Trans. Circuits Syst. I Fundam. Theory Appl.*, vol. 49, no. 8, pp. 1118–1128, Aug. 2002.
- [39] A. Zhu, J. Dooley, and T. Brazil, "Simplified Volterra series based behavioral modeling of RF power amplifiers using deviation-reduction," in *2006 IEEE MTT-S International Microwave Symposium Digest*, pp. 1113–1116, June 2006.
- [40] J. Staudinger, "DDR Volterra series behavioral model with fading memory and dynamics for high power infrastructure amplifiers," in *2011 IEEE Topical Conference on Power Amplifiers for Wireless and Radio Applications*, pp. 61–64, Jan. 2011.
- [41] J. Moon, and B. Kim, "Enhanced Hammerstein behavioral model for broadband wireless transmitters," *IEEE Trans. Microw. Theory Tech.*, vol. 59, no. 4, pp. 924–933, Apr. 2011.
- [42] P. Landin, M. Isaksson, and P. Handel, "Comparison of evaluation criteria for power amplifier behavioral modeling," in *2008 IEEE MTT-S International Microwave Symposium Digest*, pp. 1441–1444, June 2008.
- [43] M. Isaksson, and D. Wisell, "Extension of the Hammerstein model for power amplifier applications," in *ARFTG 63rd Conference, Spring 2004*, pp. 131–137, June 2004.

- [44] H. Ku, and J. S. Kenney, "Behavioral modeling of nonlinear RF power amplifiers considering memory effects," *IEEE Trans. Microw. Theory Tech.*, vol. 51, no. 12, pp. 2495–2504, Dec. 2003.
- [45] M. Isaksson, D. Wisell, and D. Ronnow, "Nonlinear behavioral modeling of power amplifiers using radial-basis function neural networks," in *IEEE MTT-S International Microwave Symposium Digest*, pp. 1967–1970, June 2005.
- [46] D. Wisell, M. Isaksson, and N. Keskitalo, "A general evaluation criteria for behavioral power amplifier modeling," in *2007 69th ARFTG Conference*, pp. 1–5, June 2007.
- [47] T. Liu, S. Boumaiza, A. B. Sesay, and F. M. Ghannouchi, "Quantitative measurements of memory effects in wideband RF power amplifiers driven by modulated signals," *IEEE Microw. Wirel. Components Lett.*, vol. 17, no. 1, pp. 79–81, Jan. 2007.
- [48] T. Liu, Y. Ye, S. Boumaiza, X. Zeng, J. He, A. B. Sesay, and F. M. Ghannouchi, "Accurate validation methods for dynamic nonlinear behavioral models of wideband RF power amplifiers using memoryless predistortion techniques," in *2007 International Symposium on Microwave, Antenna, Propagation and EMC Technologies for Wireless Communications*, pp. 358–361, Aug. 2007.
- [49] O. Hammi, "Augmented twin-nonlinear two-box behavioral models for multicarrier LTE power amplifiers," *Sci. World J.*, vol. 2014, Jan. 2014.

Vitae

Name	Mohammed Hanzala Suleman Khan
Nationality	Indian
Date of Birth	2/3/1988
Email	hanzala@kfupm.edu.sa; mhanzalakhan@gmail.com
Address	B-2/17/5, Sector-16, Vashi, Navi Mumbai-400703, India
Academic Background	B.E in Electronics Engineering, M.H. Saboo Siddik C. O. E University of Mumbai, 2010.

Work Experience

As a research assistant in the Center for Communications and Information Technology Research, Research Institute, KFUPM, I have worked on various projects such as

- **RF Radiation Measurement:** Measure and assess the RF radiation levels of Zain, STC and Mobily operators for more than 40 sites in Dammam, Al-Hasa and Al-Khobar region.
- **Narrow Band Measurement:** Using Frequency Selection Radiation Meter (NARDA SRM 3000) with Anisotropic Antenna (75 MHz- 3 GHz)-conduct field measurement comprising field intensity and power density at specific locations.
- **Scopus:** Generating statistics of publications (articles, conference papers, editorials) of universities across the Kingdom and updating it from time to time.

- **Research Tracking Application Suite:** This project involved the design and development of tab based tool for research tracking system of universities across the Kingdom of Saudi Arabia.
- **Web of Knowledge and Essential Science Indicators:** Generating statistics about highly cited researchers in various engineering disciplines.
- Performed various duties related to new applications of graduate students in the Deanship of Graduates Studies (DGS).
- Grading and proctoring the examination of undergraduate students from time to time